Summary

The research carried out under grant No. DE-FG02-07ER46371, "The State of Water in Proton Conducting Membranes", during the period June 1, 2008 -May 31, 2010 was comprised of three related parts. These are:

1. An examination of the state of water in classical proton conduction membranes with the use of deuterium T_1 NMR spectroscopy (Allcock and Benesi groups).
2. A dielectric relaxation examination of the behavior of water in classical ionomer membranes (Macdonald program).
3. Attempts to synthesize new proton-conduction polymers and membranes derived from the polyphosphazene system. (Allcock program)

All three are closely related, crucial aspects of the design and development of new and improved polymer electrolyte fuel cell membranes on which the future of fuel cell technology for portable applications depends.

Graduate Students Trained

This program has provided the support for one half of the training of one graduate student (D. Lee) to the Ph.D. level in the Allcock research group, and one quarter of the support for one Ph.D. candidate (B. O'Hare) in the Benesi group.

Publications resulting from this work

Z. Lu, G. Polizos, D.D. Macdonald, and E. Manias, "State of Water in Perfluorosulfonic Ionomer (Nafion 117) Proton Exchange Membranes", J. Electrochem. Soc, 155 (2), B163-B171 (2008).

D. Lee, H. R. Allcock, A. Benesi, D. D. Macdonald "Characterizing the State of Water in Fuel Cell Membranes Using NMR T_1 Relaxation" *Materials Research Society Fall Meeting 2008, Boston, MA* (poster abstract)

Z. Lu, E. Manias, D.D. Macdonald, M. Lanagan, "Dielectric Relaxation in Dimethyl Sulfoxide/Water Mixtures Studied by Microwave Dielectric Relaxation Spectroscopy," J. Phys. Chem. A, 113, 12207-12214 (2009).

Z. Lu, M. Lanagan, E. Manias, D.D. Macdonald, "Two-Port Transmission Line Technique for Dielectric Property Characterization of Polymer Electrolyte Membranes," J. Phys. Chem. B, 113, 13551-13559 (2009).

D. Lee, H. R. Allcock, A. Benesi, D. D. Macdonald "Polyphosphazenes for Fuel Cell Membranes" *American Chemical Society Fall National Meeting 2009, Washington DC* (poster abstract)

Z. Lu, G. Polizos, D.D. Macdonald, and E. Manias, "State of Water in Perfluorosulfonic Ionomer (Nafion) Proton Exchange Membranes", Trans. Electrochem. Soc., in press (2010). (conference paper).

Z. Lu, E. Manias, D.D. Macdonald, M. Lanagan, "Dielectric Relaxation in Dimethyl Sulfoxide/Water Mixtures", Trans. Electrochem. Soc., in press (2010). (conference

paper)

Z. Lu, M. Lanagan, E. Manias, D.D. Macdonald, “Two-Port Transmission Line Technique for Dielectric Property Characterization of Polymer Electrolyte Membranes,” Trans. Electrochem. Soc., in press (2010). (conference paper).

A. A. Argun; J. N. Ashcraft; M. K. Herring; D. K. Y. Lee; H. R. Allcock; P. T. Hammond, "on Conduction and Water Transport in Polyphosphazene-Based Multilayers," Chem. Materials, 2010, 22, 226-232.

D. Lee, "Ion Conduction Mechanisms in Polymer Electrolytes for Lithium Batteries and Fuel Cells, and Crystal Engineering of Cyclophosphazenes", *Ph.D. Thesis, The Pennsylvania State University* (2010)

D. K. Lee[1], T. Saito[2], A. J. Benesi[1], M. A. Hickner[2], H. R. Allcock[1] Characterization of Water in Proton Conducting Membranes by Deuterium NMR T_1 Relaxation, J. Phys. Chem. submitted for publication (2010).

Z. Lu and D. D. Macdonald, “Measurement of Proton Exchange Membrane Conductivity Using Dielectric Relaxation Techniques”, manuscript in preparation (2010).

Presentations

H. R. Allcock, "Proton and Lithium Diffusion in Hybrid Inorganic-Organic Polymers," International Conference on Solid State Ionics, Toronto, Canada, June 22-July 1, (2009).

Z. Lu, G. Polizos, D. D. Macdonald, and E. Manias, "State of Water in Perfluorosulfonic Ionomer (Nafion) Proton Exchange Membranes", Electrochemical Society Spring Meeting, Vancouver, B. C., Canada, April 25 - 30 (2010).

Z. Lu, E. Manias, D. D. Macdonald, M. Lanagan, “Dielectric Relaxation in Dimethyl Sulfoxide/Water Mixtures”, Electrochemical Society Spring Meeting, Vancouver, B. C., Canada, April 25 - 30 (2010).

Z. Lu, M. Lanagan, E. Manias, D. D. Macdonald, “Two-Port Transmission Line Technique for Dielectric Property Characterization of Polymer Electrolyte Membranes,” Electrochemical Society Spring Meeting, Vancouver, B. C., Canada, April 25 - 30 (2010).

General Background and Introduction

Proton Exchange Membranes (PEMs) of the type that were first introduced in the Gemini space craft about four decades ago have become an essential component of modern fuel cells. The role of the membrane is to permit the transmission of protons from the fuel side, where they are produced via the oxidation of the fuel (e.g., H_2 or CH_3OH), to the oxidizer side where they are consumed by the reduction of oxygen ($O_2 + 4H^+ + 4e^-$ to yield water). The ease with which proton transmission occurs is reflected in the potential drop across the membrane; if transmission is difficult, a high potential drop develops that subtracts substantially from the thermodynamic voltage of the cell and hence difficult proton transmission has a deleterious impact of cell power and performance.

Various previous studies for both bulk aqueous solutions and PEMs have shown that conventional proton conduction occurs via the Grotthus chain mechanism, in which the proton is passed from one water molecule to a neighboring water molecule via the rotational relaxation of the source molecule. Because water is involved in the proton conduction mechanism, the physico-chemical state of the water in the membrane and water dynamics are critically important for understanding the properties that give rise to low membrane resistivity and hence low membrane potential drop. Thus, the rotational relaxation frequency determines the rate at which protons are passed along the water "chain", and hence the rotational relaxation frequency is the key parameter for characterizing the proton conductivity. Any phenomenon or process that inhibits the free rotation of the water dipoles will decrease the conductivity.

Superimposed on these factors are the limitations imposed on fuel cell operation by the catalyst and the temperature. Expensive precious metal catalysts such as Pt or Ru function at moderate temperatures below 100^{o}C but are susceptible to poisoning by carbon monoxide. However, inexpensive metals that are less sensitive to CO require the use of higher temperatures, but the loss of water from the ionomer membrane above 100^{o}C lowers the mobility of the protons and reduces the efficiency of the cell. Because of this limitation, many investigators are exploring the possibility that adequate proton conduction within a PEM can be accomplished via alternative mechanisms that do not involve the presence of free water. To achieve this objective it is necessary to first understand the role played by water in proton conduction, and then to design membranes that function via alternative processes. This was the purpose of this work.

1. Characterization of water in proton conducting membranes in classical proton conduction membranes with the use of deuterium T_1 NMR spectroscopy:

H. R. Allcock and A. J. Benesi, with D. K. Lee (Chemistry Department), with the assistance of T. Saito and M. A. Hickner (Materials Science and Engineering Department)

Rationale

^2H T_1 NMR relaxation was used to characterize the molecular motion of deuterated water (^2H_2O) absorbed by different proton conducting membranes, which were Aquivion E87-05®, Nafion 117® and sulfonated-Radel® with ion exchange capacities of 1.05 and 1.95 mmol/g. The presence of bound water with solid character was confirmed by the dependence of the ^2H T_1 relaxation to the magnetic field of the spectrometer. By comparing the ^2H T_1 relaxations of the different membranes that were equilibrated in varying humidities, the factors that influence the state of water in the membranes were identified. At low levels of hydration, the molecular motion of ^2H_2O is affected by the acidity and mobility of the sulfonic acid groups to which the water molecules are coordinated. At higher levels of hydration, the molecular motion of ^2H_2O is affected by the phase separation of the hydrophilic/hydrophobic domains and the size of the hydrophilic domains.

Background

Proton conducting membranes are an integral component of polymer electrolyte fuel cells. The function of the membrane is to transport protons generated at the anode to the cathode where they are combined with oxygen to form water. At the same time, the membrane must separate the fuel from the oxidant as well as prevent internal short-circuiting of the cell. The high proton conductivity and excellent chemical stability of Nafion® make this material the quintessential proton conducting membrane.[1] This high proton conductivity is due to the presence of hydrophilic, sulfonate-rich domains within the membrane. Water molecules that reside in these 4- 10 nm wide hydrophilic channels conduct protons by facilitating hopping transport (Grotthuss mechanism) when the rotational mobility of water is high.[2] However, the proton conductivity of Nafion decreases drastically at low relative humidity due to loss of water. Furthermore, the flexible structure of Nafion renders it unsuitable for high temperature operation where macroscopic deformation of the membrane and disruption of the ionic domains can occur.[3-5] Thus, an incentive exists to develop alternative membranes that can perform better than Nafion across a wide range of temperatures and relative humidities.

Membranes that are able to conduct protons at low humidity will enable fuel cells to operate at higher temperatures (> 100 ˚C), which would increase the activity of the platinum catalyst and reduce poisoning of the catalyst by carbon monoxide. Moreover, higher operating temperatures allow expensive platinum catalysts to be replaced by less expensive metal oxide catalysts.[6,7] Some polymer designs that are being investigated for low humidity proton conduction incorporate heterocycles, such as imidazoles[8,9] or triazoles,[10] due to their amphotericity – their ability to donate and accept protons. However, the proton conductivity of these systems is low because the rate of proton conduction is dependent on the dynamics of the larger donor-acceptor molecules. Another approach to low humidity proton conductivity is to synthesize ion containing block copolymers which form distinct hydrophobic and hydrophilic phases due to the presence of a highly sulfonated hydrophilic block and a hydrophobic block.[11-15] The function of the hydrophobic phase is to provide mechanical stability to the hydrophilic, sulfonated phase, which would have poor mechanically stability when hydrated. The proton conductivities of these block copolymers are comparable to Nafion when hydrated, but an improvement over Nafion at low humidity is difficult to attain.[11]

Many studies on the nanophase structure of proton conducting membranes have been carried out to correlate the size and connectivity of the hydrophilic domains with proton conductivity.[1,16-18] However, the characterization of water that is absorbed in the membrane is equally important since water is the proton conducting medium. The nature of water in proton conducting membranes has been probed using different techniques such as dielectric spectroscopy,[19,20] differential scanning calorimetry,[21,22] infrared spectroscopy,[23] and nuclear magnetic resonance.[24,25] Computational methods have also been used to model the molecular motions of water in proton conducting membranes.[26,27] It has been proposed (and this is still controversial) that at least two types of water are present in fuel cell membranes which are termed 'free' water and 'bound' water. 'Free' water is essentially water that exists within the hydrophilic pores of the membrane which is uncoordinated to the polymer and displays characteristics that are similar to bulk water. On the other hand, 'bound' water is strongly coordinated to the sulfonic acid groups of the polymer. Due to its limited mobility, bound water has characteristics that resemble solid water at room temperature and this form of water has been reported in various systems including inorganic solids[28-30] and polymer systems.[31,32] Studies have shown that the 'bound' water molecules are difficult to remove by heating because of their strong coordination to the sulfonic acid groups.[33] Hence, it is conceivable that bound water can be used in a highly sulfonated polymer system for proton conduction at high temperatures. Proton conduction can occur through a mechanism similar to that in ice which involves Bjerrum defects and tetrahedral jumps of the bound water molecules.[34] Therefore, understanding the state of water in relation to the chemical structure of the polymer and the morphology of the membrane will provide valuable information for planning the synthetic strategy of future proton conducting polymers.

The purpose of this study was to characterize the molecular motion of water molecules that are absorbed in proton conducting membranes. Different proton conducting polymers were chosen with varying chemical and morphological properties that should influence the molecular motion of water that is absorbed. ^{2}H NMR T_1 relaxation was used to probe the molecular motion of deuterated water (^2H_2O) that was used to hydrate the membranes. ^{2}H T_1 relaxation measurements have an advantage over other techniques because they allow *direct* observation of the molecular reorientational dynamics of the ^{2}H-O bond. Furthermore, consideration for the intermolecular dipolar interactions is not required, as opposed to ^{1}H NMR experiments.[35,36] In an NMR T_1 relaxation or spin-lattice relaxation experiment, the nuclei are excited to a higher energy state by a radio frequency (RF) pulse. The measured relaxation time is the average lifetime of the higher energy state. In other words, it is the time needed for the higher energy nuclei to dissipate their energy into the lattice. The ^{2}H T_1 relaxation of solid water is short because the molecular motions of solid water occur at frequencies comparable to the Larmor frequency of the nuclei. Therefore, the energy transfer is efficient and the nuclei relax in about 3 to 10 ms, depending on the magnetic field of the spectrometer. The field dependence of the ^{2}H T_1 relaxation is due to the different Larmor frequencies. By contrast, the ^{2}H T_1 relaxation of bulk water is 400 ms and does not show a dependence on magnetic field because the molecular motion is much faster than the Larmor frequency, and thus energy dissipation from the excited nuclei is inefficient. In work that preceded this project, Benesi was able to characterize the state of water in ^2H_2O-hydrated inorganic porous solids, such as Zeolite A and kanemite, using ^{2}H T_1 relaxation measurements.[28-30] The ^{2}H T_1 relaxation of these hydrated inorganic solid

were 3 to 10 ms at room temperature, depending on the magnetic field of the NMR spectrometer, which indicates that ^2H_2O is in the solid state. Using the same principles, we have used NMR T_1 relaxation to characterize the state of water in proton conducting membranes.

Experimental Technique

Membrane Materials. Nafion 117 was purchased from Ion Power Inc. Aquivion E87-05 and Radel (R-5500, M_W 63 kg/mol) were kindly donated by Solvay Solexis. Radel was sulfonated using a modified reference procedure.[37]

Cleaning Procedure. All membranes samples were cut into strips (approximately 3 mm x 35 mm) and were treated to an extensive cleaning procedure prior to NMR analysis. Paramagnetic impurities in commercial membranes were a particular concern because these can shorten T_1 relaxation times and hence distort the interpretation of the data.[25] The procedure was:

i. 24 hour soak in ethanol:water (1:1) solution
ii. Rinse in distilled-deionized (*dd*) water
iii. Boil in 3% hydrogen peroxide for 1 hour
iv. Rinse in *dd* water
v. Boil in 2 M H_2SO_4 for 2 hours
vi. Rinse in *dd* water three times
vii. Drying under vacuum at 80 °C for 24 hours.
viii. Soak in D_2O

In-Situ NMR Tube Hydration. The proton conducting membranes were hydrated within an NMR tube using a method similar to the one described by Perrin.[38] Membranes were placed at the bottom of the NMR tube. A porous separator was placed above the membrane strips and a small tube (3 mm *OD* x 1.5 mm *ID* x 50 mm *L*) containing a saturated salt solution of ^2H_2O was inserted to control the humidity within the NMR tube.[39] The tubes were sealed with epoxy cement and allowed to equilibrate over a minimum period of 3 weeks. To ensure full equilibration of the membrane, the NMR relaxation measurements were repeated until a consistent value was obtained. Equilibration times were shorter if the membrane started from a hydrated state as opposed to a dried state because the rate of desorption of water is an order of magnitude faster than rate of sorption of water,[40] although, both routes ultimately gave the same ^2H T_1 relaxation times.

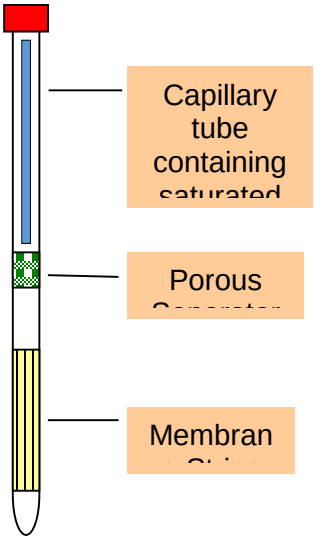

Figure 1 Experimental setup for *in-situ* humidification

NMR T_1 Relaxation Experiments. ^{2}H NMR experiments were carried out over a range of temperatures at four magnetic fields, specifically at 7.0, 9.4, 11.7, 14.1 Tesla, on four different NMR spectrometers: a homebuilt solid state Tecmag-300, a solid state Chemagnetics/Varian Infinity 500, a liquid state Bruker DPX-300, a liquid state Bruker DRX-400, a liquid state Bruker AV-3-500, and a liquid state Bruker AV-3-600 at a range of carefully calibrated temperatures (± 1 K).

The quadrupole echo pulse sequence, $(\pi/2)_x$-τ_1-$(\pi/2)_{\pm y}$-τ_2-Acquire$_x$ with Cyclops phase cycling was added to all pulse phases and the receiver phase, was used to obtain ^{2}H spectra on the solid state Tecmag-300 and Infinity 500 spectrometers at 45.65 and 76.77 MHz respectively ($\pi/2$ = 1.8 to 2.5 μsec, τ_1 = 30 μsec, τ_2 = 25 μsec, spectral width = 1 MHz). The T_1 value of the sharp central aqueous peak was determined at various magnetic fields as a function of temperature with the inversion recovery pulse sequence, π_x - $\tau_{variable}$ – $(\pi/2)_{\phi 1}$ - Acquire$_{\phi ref}$, with ϕ1 = x, y, -x, -y and ϕref = x, y, -x, -y, or the inversion recovery quadrupole echo experiment, π_x - $\tau_{variable}$ – $(\pi/2)_x$-τ_1-$(\pi/2)_{\pm y}$-τ_2-Acquire$_x$ (with Cyclops). At temperatures where the central peak is sufficiently sharp, $\Delta\nu_{1/2}$ < 5 kHz, the data from liquid state spectrometers were obtained using relatively "soft" pulses on a liquid state probe with $\pi/2 \approx 13$ μsec and $\pi \approx 26$ μsec. As verified by separate experiments with hard pulses ($\pi/2 \leq 2.5$ μsec) on the solid state Tecmag-300 and Infinity-500 spectrometers, the pulses using the liquid-state probe were adequate for uniform excitation of the sharp central peak at temperatures where it could be resolved. Variable temperature quadrupole echo spectra were obtained on the solid state Tecmag-300 and Infinity 500 spectrometers using a Chemagnetics variable temperature apparatus. The temperature was calibrated with a copper constantan thermocouple taped in place inside the empty sample coil of the intact probe/variable temperature apparatus operating inside the magnet. The temperatures reported on these instruments are accurate to ca. ± 1 K throughout the reported temperature range.

Water Uptake and Proton Conductivity. The membranes were equilibrated at 25 ˚C in an Espec SH-241 humidity chamber to measure the proton conductivity and water uptake. The proton conductivities of the membranes were measured by two-probe electrochemical impedance spectroscopy (EIS) using a Solartron 1260A frequency response analyzer coupled to a Solartron 1287 potentiostat. The isothermal water uptake of the membrane was converted to hydration number by the equation, λ = [mass of absorbed water/(dry mass of membrane × IEC × molecular mass of water)].

Results and Discussion

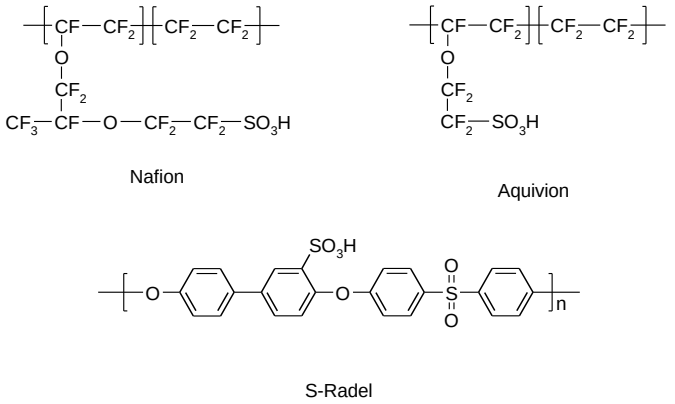

Figure 2. Structures of proton conducting polymers examined in this work

Overview of Membranes

Nafion and Aquivion are perfluorosulfonic acid/polytetrafluoroethlene copolymers (PFSA), which are manufactured by Dupont and Solvay Solexis respectively. Nafion has been the mainstay in fuel cell studies for many years.[1] Recently, there has been rising interest in PFSA polymers with short side chains due to the better mechanical properties and performance in fuel cells.[41] Aquivion, also previously known as Hyflon Ion, is in many respects structurally similar to Nafion except that the sulfonic acid group is tethered to a shorter side chain (-O-C-C-) instead of a longer side chain (-O-C-C-O-C-C-). The Dow Chemical Company also manufactured a short side chain PFSA membrane, which has been discontinued. Although the Nafion and Aquivion membranes that were used in this study have different equivalent weights, 1100 and 870 grams/mole respectively, the average separation between sulfonic acid-containing monomers along the backbone chain differs only by one CF_2CF_2 repeat unit.

Radel is a poly(arylene ether sulfone) which is also manufactured by Solvay Solexis. It can be post-sulfonated to form robust proton conducting membranes with aryl sulfonic acid groups on the main chain. The rigid aryl backbone gives Radel a high glass transition temperature (T_g) but it is less hydrophobic than a fluorinated polymer. As an aromatic hydrocarbon polymer, Radel is lower in cost and has less environmental concerns compared to fluorinated polymers, and is thus more accessible depending on the desired proton conducting membrane properties. Two sulfonated-Radel (S-Radel) membranes with two ion exchange capacities (IEC) of 1.05 and 1.95 mmol/g are compared in this study and

will be referred to as S-Radel 1.05 and S-Radel 1.95. The relevant properties of the different polymers and their membranes are summarized in Table 1.

Table 1 Property comparisons of different proton conducting membranes

Polymer	IEC (mmol/g)	Backbone	T_g (˚C)	Acidity (pKa)	Side Chain (atoms)	Phase Separation
Nafion 117	0.91	Perfluorinated alkyl	120	-6	6	Distinct
Aquivion E87-05	1.14	Perfluorinated alkyl	160	-6	3	Distinct
S-Radel	1.05 & 1.95	Hydrocarbon aryl	220	-1	0	Poor

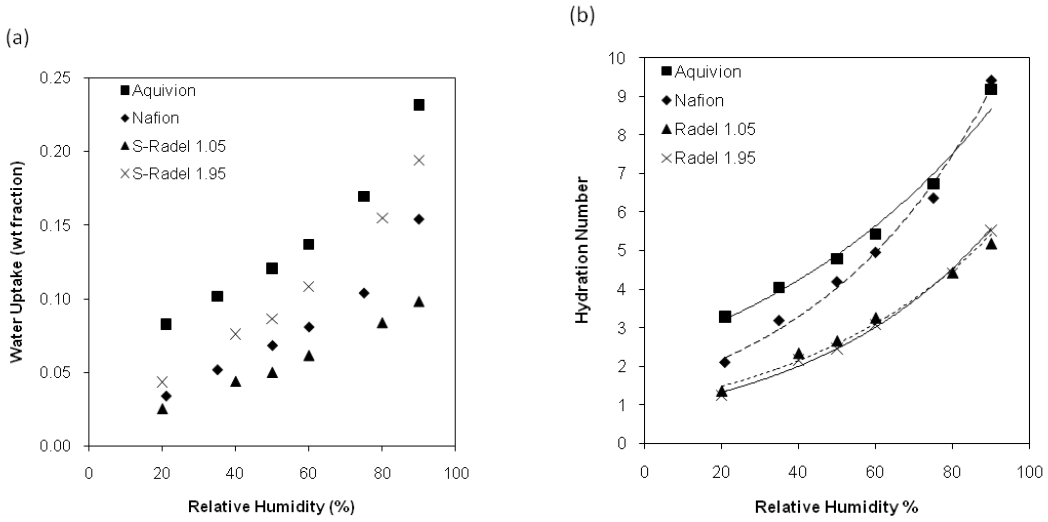

Figure 3 (a) Water uptake and (b) hydration number of proton conducting membranes with respect to humidity

Water Uptake Behavior

The proton conducting membranes were equilibrated at different relative humidities and the water uptake was measured. The hydration number, λ = (mole H_2O absorbed/mole SO_3H) for each condition was also calculated. The amount of water absorbed by the proton conducting membranes was controlled by the humidity of the environment in which the sample is equilibrated.[42] Water uptake of the proton conducting membranes showed increasing water uptake with increasing relative humidity. The weight fraction of water absorbed by S-Radel 1.95 was higher than S-Radel 1.05 due to the higher IEC of S-Radel

1.95. However, the hydration numbers of the both S-Radel samples at a given humidity level were similar. The same observation can be applied to Aquivion and Nafion membranes. In general, the PFSA membranes absorbed more water than the S-Radel membranes because of their flexible backbone structures and larger hydrophilic channels.[16] Construction of a correlation curve of hydration number versus humidity allows an estimation of the hydration number of the membranes equilibrated in the NMR tubes at a given humidity.

Presence of Bound Water

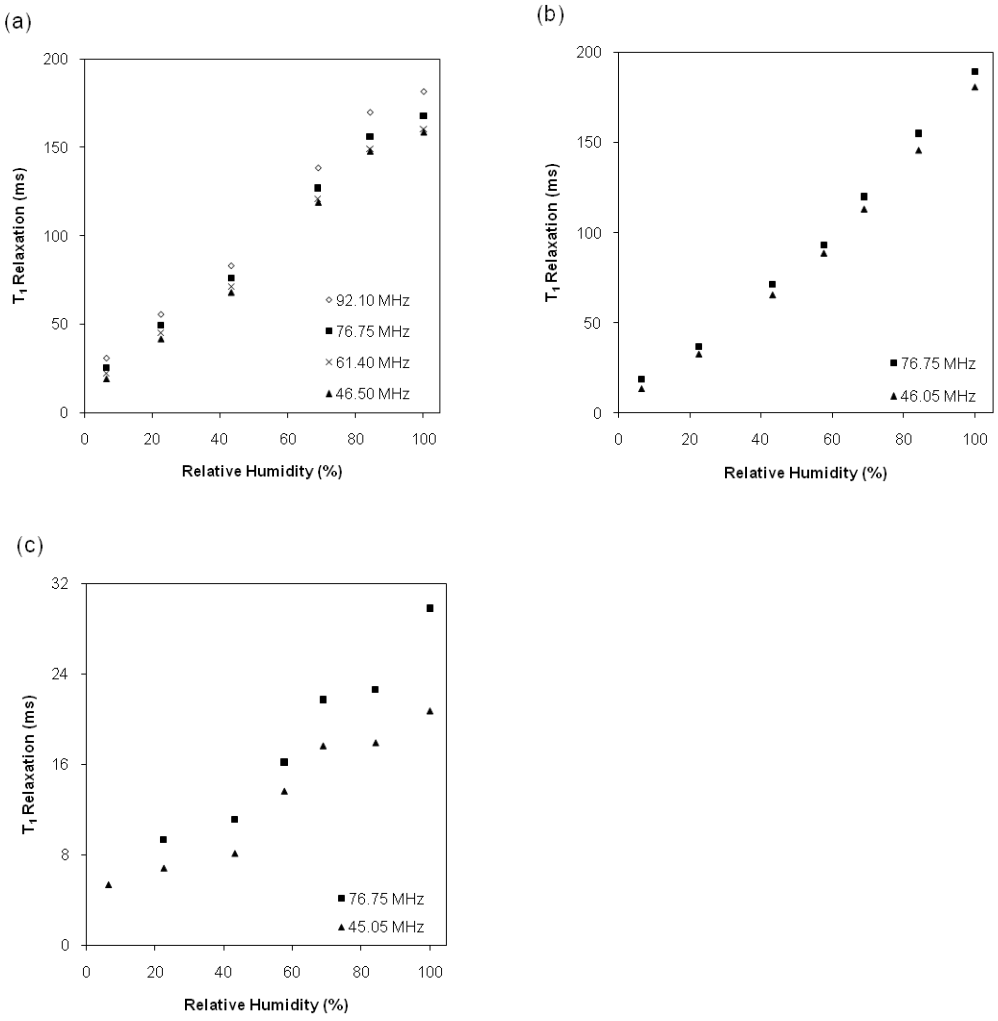

Figure 4 ^{2}H T_1 relaxation times of ^2H_2O in (a) Nafion, (b) Aquivion, and (c) S-Radel 1.95 at different magnetic fields at 25 ˚C.

The ^{2}H T_1 relaxation times of ^2H_2O that was absorbed by the proton conducting membranes at various humidities were obtained at different magnetic fields at 25 ˚C. The ^{2}H Larmor frequency in the magnetic fields of the spectrometers used were 92.13, 76.77, 61.42, and 46.07 MHz. Figure 4 shows that T_1 relaxation in Nafion and Aquivion increases rapidly in a somewhat linear fashion relative to the humidity in the tube. Conversely, the

increase in ^2H T_1 relaxation with humidity of S-Radel 1.95 was much smaller than the PFSA membranes and it shows an inflection point at around 55% RH. At low humidity, the amount of absorbed water is small and it is bound to the sulfonic acid groups as waters of hydration. These 'bound' water molecules have characteristics of solid water, and therefore the ^2H T_1 relaxation is short. As the humidity level increases, 'free' water becomes present as more water is absorbed by the membrane and it is characterized by longer T_1 relaxations times. Furthermore, ^2H T_1 relaxation times of the same membrane samples measured at higher magnetic fields were also longer, indicating the presence of bound water in every membrane sample.[30] Only one resonance peak was detected in the NMR spectrum. When fit with the Kohlrausch exponential function, the T_1 relaxation data obtained yield $\beta \geq 0.99$, consistent with monoexponential relaxation or a narrow range of relaxation times.[43] The monoexponential decay is consistent with rapid exchange between the different types of water.[44]

^2H T_1 Relaxation Behavior of Different Membranes

In order to correlate the state of water to the chemical and morphological structure of the different proton conducting membranes, the ^2H T_1 relaxation at 46.05 MHz was plotted against the hydration number of the membranes that were equilibrated in different relative humidities (RH) according to the saturated salt solutions in the tube. The hydration number for each membrane was estimated by a logarithmic equation that was used to fit the λ versus RH curves of each membrane in Figure 3b. The hydration number was used instead of relative humidity to compare the ^2H T_1 relaxations of the different membranes because of the different water uptake behavior of each proton conducting membrane. There were significant differences between the ^2H T_1 relaxation curves of the different membranes. The ^2H T_1 relaxation times of Nafion and Aquivion range from 19 – 148 ms and 13 – 145 ms respectively whereas the ^2H T_1 relaxation times of the S-Radel 1.05 and S-Radel 1.95 ranged from 5 – 22 ms only. Furthermore, there was an inflection point around $\lambda = 3$ for the ^2H T_1 relaxation curves for S-Radel membranes which was not detected in PFSA membranes. The relationship between the chemical and morphological structure of the proton conducting membranes to the ^2H T_1 relaxation behavior is discussed below.

The ^2H T_1 relaxations of the S-Radel membranes at low humidity are comparable to previously reported systems such as kanemite and Zeolite A.[28-30] We have carried out experiments on freeze dried starch and cellulose that was hydrated with ^2H_2O which also showed ^2H T_1 relaxations of 5 ms at 45.05 MHz.i However, the ^2H_2O in Aquivion and Nafion membranes exhibit long ^2H T_1 relaxation times at low hydration, 13 ms and 19 ms respectively. The unusually long ^2H T_1 relaxation in Nafion at low hydration has been reported previously.[25,44a,b]

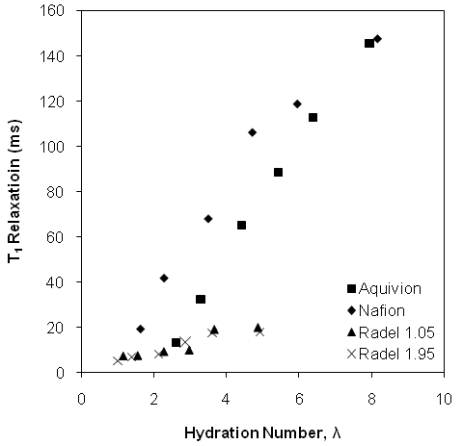

Figure 5 ^{2}H T_1 relaxation times at 45.05 MHz for different proton conducting membranes with hydration number.

There are two possible reasons for the longer ^{2}H T_1 relaxations in PFSA membranes at low hydration. First, the acidity of the sulfonic groups in the PFSA membranes is higher than in S-Radel.[16] The sulfonic acid groups in Nafion and Aquivion are attached to a perfluorinated alkyl chain which has highly electronegative fluorine atoms that withdraw electron density from the sulfonate group, thus stabilizing the negative charge. The acidity of the sulfonic acid group in S-Radel is not as high as in the PFSA membranes because the negative charge of the sulfonate ion is merely delocalized on the aryl ring.[48] Therefore, the water molecules coordinate more strongly to the aryl sulfonic acid group because it has a higher electron density than the perfluorinated sulfonic acid group. Using *p*-toluene sulfonic acid and triflic acid as analogues, computer modeling predicted that the distance between the sulfonic acid groups and the hydrating water molecules is closer for para-toluene sulfonic acid than for triflic acid,[48] which supports our hypothesis. Secondly, the sulfonic acid groups are attached to flexible side chains in PFSA membranes whereas the sulfonic acid groups in S-Radel are attached directly to a rigid polymer backbone. This may be a contributing factor to the higher ^{2}H T_1 relaxations in PFSA membranes because the sulfonic acid groups in PFSA membranes have more mobility than in S-Radel, and could affect the molecular motion of the water that is coordinated to the sulfonic acid groups. The side chain motion may also explain the slightly shorter ^{2}H T_1 relaxations in Aquivion, which has a shorter side chain than Nafion.

The chemical structure of the polymer influences the ^{2}H T_1 relaxation behavior at low hydration levels. However, influence from the morphological structure of the membrane becomes more important as the hydration level is increased. When $\lambda \approx 4$, the S-Radel membranes showed a sudden increase of 10 ms in the ^{2}H T_1 relaxation which is attributed to the saturation of the hydration shell of the sulfonic acid groups and/or the onset of the formation of hydrophilic domains. The sudden increase in ^{2}H T_1 relaxation time can also be linked to the proton conductivity behavior of the S-Radel samples. When λ is less than four, the S-Radel 1.95 membrane exhibits very low proton conductivity while the S-Radel 1.05 membrane has no measureable conductivity. When λ reaches four, 'free' water

becomes present and interconnected pores may be formed. Hence, proton conductivity increases more rapidly for S-Radel 1.95 and there was measureable conductivity from S-Radel 1.05. IEC does not appear to have a major influence on ^2H T_1 relaxations of the S-Radel membranes as the difference between the two ^2H T_1 relaxation curves is minor.

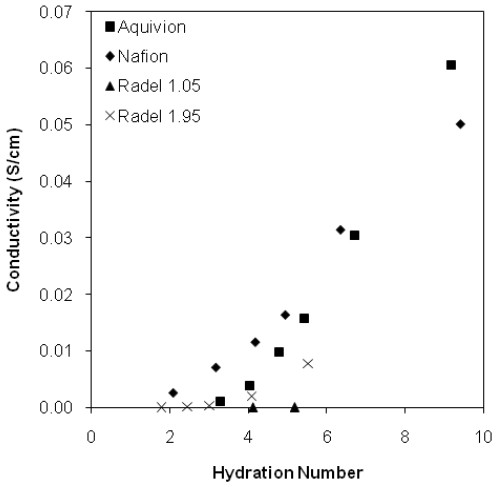

Figure 6 Conductivity versus hydration number of the different proton conducting membranes

The effect of morphology on the ^2H T_1 relaxation behavior is more apparent in PFSA membranes. The ^2H T_1 relaxations of PFSA membranes are long, even at relatively low levels of hydration. Moreover, there is no observable inflection point in the ^2H T_1 relaxation curve of PFSA membranes as the hydration number increases. The lack of an inflection point may be due to sulfonate rich domains being already present in PFSA membranes even in the dry state, which can be detected by TEM and SAXS methods,[49,50] and therefore distinct hydrophilic domains are formed at minimal hydration. Furthermore, the more flexible and hydrophobic nature of the fluorinated alkyl backbone of PFSA polymers aids in the formation of well defined phase-separated domains with large hydrophilic pores (5 nm). Therefore, water molecules that are absorbed in PFSA membranes have more liquid character, and consequently give rise to longer ^2H T_1 relaxations. Conversely, the backbone of S-Radel is very rigid and less hydrophobic than the PFSA polymers, which leads to poor phase separation between the hydrophilic and hydrophobic phases, and formation of much smaller hydrophilic pores. The water molecules confined in small pores exhibit more solid character because their molecular motion is restricted.

Conclusions

The state of water within proton conducting membranes has been characterized by measuring the ^2H T_1 relaxation of ^2H_2O within the membranes stucture. The chemical and morphological properties of the polymer that influence the molecular dynamics of water molecules absorbed by proton conducting membranes were identified. The acidity and mobility of the sulfonic acid groups have the most influence on the character of the water at low hydration levels. Phase separation and pore size of the hydrophilic domains have

more influence on the state of water at higher levels of hydration. In the future, ^2H T_1 relaxations of ^2H_2O in aromatic ionomers with highly sulfonated blocks that form large hydrophilic domains, rigid poly(arylene ether)s with flexible sulfonic acid groups, and sulfonated polyphosphazenes which have a highly flexible backbone will be investigated in order to confirm our hypothesis. Understanding the character of water in proton conducting membranes will provide vital information for the design of future systems, especially ones that rely on bound water to conduct protons, which perhaps can operate at high temperatures and low humidity.

2. A dielectric relaxation examination of the behavior of water in classical ionomer membranes

D. D. Macdonald: Materials Science and Engineering Department

No funds were allocated in this project for student support in the Department of Materials Science and Engineering and, consequently, no new DRS measurements could be made. Instead, Dr. Macdonald used the resources that were available to analyze DRS data that had been collected, but not fully analyzed, in a previous DOE-funded project [Subcontract No. 3540OB via Contract No. DE-FC04-02AL67608 through International Fuel Cells (IFC) Inc.] and to prepare seven publications for prestigious, peer-reviewed journals. Three papers were also presented at the Spring Meeting of The Electrochemical Society, April 25 – 30, 2010, in Vancouver, B.C., Canada. Assisting the author in this task were Dr. Zijie Lu, who received his Ph.D. on above subcontract, Professor Evangelos Manias, Professor Michael Lanagan, and Dr. George Pozlios (Post Doctoral Fellow on the IFC subcontract). Professor Manias also acknowledges support from the National Science Foundation (NSF grant # DMR-0602877).

Below is a summary of the work carried out by Macdonald and his colleagues on three subtasks. The discussion of each subtask begins with a statement defining the problem and the approach taken in resolving the issues, followed by a brief statement of the findings. More detailed accounts can be found in the papers listed in the "Publications" section of this report.

Introduction.

One of the most reliable methods for interrogating the state of water in ionomer membranes is dielectric relaxation spectroscopy (DRS) operating in the microwave region of the electromagnetic spectrum. By measuring the complex dielectric constant over the requisite frequency range, it is possible to ascertain the relaxation frequencies of the various types of water ("free" water, "loosely-bound" water, and "strongly-bound" water) in the membrane.

Two Port Transmission Line Method for Measuring Dielectric Relaxation Spectra

Perfluorosulfonic acid (PSA) polymer electrolytes have attracted much attention over the past decade because of their wide applications in polymer electrolyte membrane fuel cells (PEMFC) as well as in other electrochemical devices such as electrochemical

sensors and water electrolyzers.[51-53] Especially, their application in PEMFCs has led to extensive research of their structure-property relationships. Nafion (a DuPont registered trademark polymer) has become the prototypical polymer electrolyte, because of its high proton conductivity along with the highly stable chemical, mechanical, and thermal properties. Nafion naturally combines, in one molecule, a hydrophobic backbone and hydrophilic sulfonic acid functional side groups, which promote a microphase separation between the polar (hydrophilic) and nonpolar (hydrophobic) constituents.[54,55] In its hydrated form, Nafion's hydrophilic (nano)phases contain water and acidic groups and can become interconnected to provide pathways for the transport of dissociated protons; concurrently, the hydrophobic domains consist of the fluorocarbon backbone and provide good mechanical and thermal stability. The structure and morphology of Nafion have been reported in several comprehensive reviews. [56,57]

PSA membranes are essentially aqueous electrolytes because they are only operational when sufficient amount of water is absorbed around the sulfonic acid groups. This particular feature enables the use of dielectric relaxation spectroscopy (DRS), which monitors the cooperative motion of molecular assemblies, providing a powerful tool for the characterization of these materials. DRS probes the response of the total dipole moment of a system, $M(t) = \mu_i(t)$ inside a time-dependent external electrical field; represents the individual molecular dipole moments. The dielectric properties of a material is described by the complex relative permittivity spectrum,

$$\varepsilon^*(\omega) = \varepsilon'(\omega) - j\varepsilon''(\omega) \qquad (1)$$

$$j = \sqrt{-1}$$

As noted above, the dielectric properties of polymer electrolytes can yield important information on the molecular structure of the system and the physical state of water in these materials.[58-61] Furthermore, the dielectric relaxation behavior provides insight on the impact of the polymer environments on the cooperative solvent dynamics, which have important ramifications on water and proton transport in these membranes.[62-65] It is widely accepted that water confined in systems such as reverse micelles possess different dynamics compared to bulk/free water. As structural diffusion (i.e., the Grotthuss mechanism) of protons in bulk water requires coordinated formation and cleavage of hydrogen bonds of water molecules in the second hydration shell of the hydrated proton (Zundel and Eigen ions,[66,67]), and requires rotational relaxation, any constraint to the dynamics of the water molecules will decrease the mobility of the protons.

However, despite their obvious importance, the available dielectric data for PSA polymer electrolytes are rather limited. Mauritz and coworkers[68,69] reported constant temperature dielectric relaxation analyses of Nafion membranes imbibed with various ions attempting to model long range ion transport. Tsonos et al.[70,71] studied the dielectric relaxation of K^+ exchanged Nafion at 25 ^oC. These investigations were limited to low frequencies (f < 10 MHz). However, for aqueous electrolytes around ambient temperature, the frequencies for dielectric relaxation are in the microwave region, which requires special instrumentation. The high specific electric conductivity of these systems presents another challenge because only the total loss of the sample is experimentally accessible;

$$\eta''(\omega) = \varepsilon''(\omega) + \eta''_{\sigma} = \varepsilon''(\omega) + \frac{\sigma}{\omega\varepsilon_0} \quad (2)$$

ε_0 is the permittivity of the vacuum. Obviously, the Ohmic loss dominates the total dielectric loss below a minimum frequency, which is characteristic of each system, and in the case of hydrated PSA usually lies in the radio frequency (RF) and microwave frequency range, thus limiting the spectral range accessible to experiments. [11] Therefore, there is an increasing demand for accurate, high frequency (microwave) dielectric characterization techniques capable of robust measurement of the dielectric properties of various electrolytes including aqueous and polymeric materials.

Currently, there are numerous available microwave dielectric property measurement techniques. The open-ended coaxial probe technique enables convenient and nondestructive measurements of the dielectric properties of infinite half-space solids and liquids,[72-74] and has been extended to the measurements of finite-thickness layered materials.[72,75] In a recent work, Paddison et al.[76,77] used the technique to measure the dielectric properties of Nafion 117 in the frequency range of 0.045–30 GHz. However, no detailed information about discrete water relaxations were obtained although their results showed a strong dependence of the dielectric constant and of the loss factors on the water content. In this case, a planar measurement surface is required. Moreover, improper contact between the probe aperture and the material surface can result in significant errors in measuring its dielectric properties. Resonant cavity methods render accurate measurements, but they are not broadband and are generally limited to low loss values (*tan* < 0.02). On the other hand, transmission line techniques are relatively accurate measuring the broadband dielectric properties of intermediate and high loss dielectric materials. Of these, the two-port transmission line techniques[78,79] are presently widely used. In general, these techniques make use of the reflected and/or transmitted waves by and through a dielectric-filled transmission line in order to analytically or numerically determine the dielectric properties of the material. In addition, the two-port transmission line techniques are well suited for the dielectric measurement of polymer electrolytes. In this case, a precisely cut sample is placed in a section of transmission lines and the complex scattering parameters are measured over a wide frequency range. The scattering equations relate the reflected/transmitted waves to the permittivity and permeability of the material. The dielectric properties of a material are then determined analytically or numerically from the relevant scattering parameters.

In our previous work, we have studied the dielectric relaxation spectroscopy of Nafion 117 combining normal broadband dielectric spectroscopy and two-port microwave transmission line method; there we identified at least two water relaxation mechanisms in the microwave frequency range within the hydrated membrane, in addition to the slower modes of water in the hydration shells around the acidic groups.[61] In this work, the emphasis is on further development of this microwave frequency transmission technique, including examining the scattering equations in detail, presenting a simplified iterative numerical method for obtaining the dielectric spectra, and validating the technique using pure water and PTFE film whose dielectric properties are well known. A second goal of the work is to investigate the dielectric relaxation behavior of an additional PSA membrane having different equivalent weight (EW) than Nafion-11x. It is believed that EW is an

important factor in determining the structure of the membrane and the dynamics of protons and water molecules within the membrane. For this purpose, the dielectric spectra of Flemion SH 150, which has a similar chemical structure to Nafion 117, but has a lower equivalent weight (EW= 909 g/equiv vs. EW=1100 for Nafion-11x), were measured using the two-port transmission line technique and compared with those of Nafion 117.

As noted above, with the ever increasing utilization of perfluorosulfonic acid membranes, such as Nafion and Flemion, there is a growing demand for dielectric characterization of these materials towards a quantitative understanding of the dynamics of water molecules and protons within the membranes. In this work, a two-port transmission line technique for measuring the complex permittivity spectra of polymeric electrolytes in the microwave region is described and the algorithms for permittivity determination are presented. The technique is experimentally validated with liquid water and polytertrafluoroethylene film, whose dielectric properties are well-known. Using this technique, the permittivity spectra of dry and hydrated Flemion SH150 membranes are measured and compared with those of Nafion 117. Two water relaxation modes are observed in the microwave region (0.40–26 GHz) at 25 ^{o}C. The higher-frequency process observed is identified as the cooperative relaxation of free/bulk-like water, whose amount increases linearly with increasing water content in the polymer. The lower-frequency process, characterized by longer relaxation times in the range of 20-70 picoseconds, is attributed to water molecules that are loosely bound to sulfonic acid groups. The loosely bound water increases with increased hydration and levels-off at higher water contents. Flemion SH150, which has an equivalent weight of 909 g/equiv, displays higher dielectric strengths for both of these water modes than does Nafion 117 (equivalent weight of 1100 g/equiv), which may indicate the effect of the equivalent weight on the polymer structure, and in particular on the ionic cluster regions. A full account of this work may be found in Z. Lu, M. Lanagan, E. Manias, D.D. Macdonald, "Two-Port Transmission Line Technique for Dielectric Property Characterization of Polymer Electrolyte Membranes," *J. Phys. Chem. B*, **113**, 13551-13559 (2009).

State of Water in Nafion Membranes

Increasing interest in studies of proton exchange membranes (PEMs), mostly Nafion® membranes, is inspired by their active application in proton exchange membrane fuel cells (PEMFC), which are considered to be the most promising power source for future automotive and stationary applications.[80] The water content of the PEMFC is of major importance, due to its influence on properties, such as proton conductivity[81,82], methanol permeability[83-85], and electro-osmotic drag.[86,87] The most frequent application of Nafion membrane is to perform as both a separator and an electrolyte in electrochemical cells, including fuel cells and chlor-alkali cells, and hence, the overall function of the cells is influenced strongly by the conductivity of the membrane, which is achieved by proton transportation through the membrane. Proton conduction in Nafion is generally believed to occur via the Grotthus chain mechanism, in which a proton is passed between adjacent water molecules through a cooperative rotation/proton transfer process. Due to the strong ion-dipole and dipole-dipole interactions between the water molecules and various polar groups (most notably, $-SO_3^-$), the structural and dynamical properties of nano-confined water are distinct from bulk water. Different water states have been proposed to exist in

Nafion membranes. On the basis of X-ray diffraction studies, Gierke et al.[88,89] proposed that water and counter ions form spherical clusters with diameters of 30-50Å. Falk[90] concluded, from infrared studies, that a significant amount of water in the clusters is associated with the fluorocarbon phase. A significantly reduced hydrogen bonding strength has been observed for water absorbed into Nafion compared with that for bulk liquid.[90,91] Two water environments have therefore been postulated as being associated with a void volume and an ion cluster region.

In polymers, mainly in hydrogels, by the use of differential scanning calorimetry (DSC) measurements, three types of water have been proposed, depending on water/polymer interactions:[92-95] a) Bulk like water that does not interact with the polymer matrix and exhibit melting endothermic peak at 0°C; b) water that interacts weakly with the polymer and exhibits broad endothermic peak below 0 °C and c) water that strongly interacts with the polymer and does not freeze. Specifically, on hydrated Nafion membranes, DSC studies[96] also reveal at least two types of water molecules: Mobile and immobilized water. The immobilized molecules were supposed to be either strongly bound to $-SO_3^-$ groups or entrapped in the fluorocarbon backbone.

Dielectric relaxation spectroscopy (DRS) probes the response of the total dipole moment of a system, , to a time-dependent external electrical field. This inherent ability to monitor the cooperative motion of a molecular ensemble makes it a powerful tool for investigating liquids, whose structure and dynamics is dominated by intermolecular hydrogen bonds. Several dielectric relaxation studies have been reported at relatively low frequencies (f < 10MHz). Mauritz and Deng[97] reported a conductivity contribution and a bimodal relaxation in the low-frequency region of log () vs. log () plots, and suggested that the observed response was due to the existence of two types of hydrated clusters. Pissis et al.[98] reported a dielectric relaxation occurring at 50kHz at 25°C in Nafion-K membranes ($-SO_3K$), which was attributed the rotation of ($-SO_3^-$) group-water complexes at the end of the side chains. However, these investigations do not provide a clear description of the state of water within the membranes. In attempting to elucidate the state of water in proton exchange membranes, Paddison *et al*.[99] measured the dielectric spectrum of Nafion 117 in the microwave region (0.045-30GHz). Their results showed a strong dependence of the dielectric constant and loss factor on the water content. Specific information concerning the state of water in these membranes could not be obtained from their work, because of the poor quality of the data.

In view of the inconclusive results concerning the structure of water in Nafion membranes, it is appropriate to investigate the temperature dependence of the dielectric spectra of variously hydrated Nafion membranes. Accordingly, we report here a dielectric relaxation study of hydrated Nafion 117 in the acid form over wide frequency and temperature ranges (0.045-26GHz, 25°C to 45°C) and (10^{-2}-10^7Hz, 25°C to -50°C). The specific objectives of the work are to characterize the state of water in the membranes, in order to understand better the mechanisms of proton conduction and the dependence of other properties (e.g., swelling) influenced by the presence of water in the polymer.

Complex dielectric permittivity spectra, of Nafion 117 membranes, in the acid form ($-SO_3H$), at several hydration levels have been measured by using the transmission line method over the frequency range of 0.045-26GHz (25°C to 45°C) and broadband dielectric

relaxation spectroscopy 10^{-2}-10^{7}Hz (25°C to -50°C). The spectra generally show two Debye relaxation processes for water in the GHz range. The highest-frequency process exhibits the characteristic dynamics of bulk water, and is attributed to the cooperative relaxation of hydrogen-bonded networks of "free" water in the membrane. At lower frequencies a second process is observed, which is attributed to water molecules in the second hydration shell around the sulfonic groups or to water of hydration of hydrophobic entities (e.g., -CF_3 groups). In agreement with other investigations, a slow relaxation mode (10^{-2}-10^{7}Hz) was also observed, being postulated to result from the rotation of the sulfonic groups associated with water molecules, forming thus the first hydration layer. Because proton conduction is generally considered to occur in aqueous systems via the Grotthus chain mechanism, which involves cooperative molecular (water) rotation and proton transfer, and since the rotational relaxation frequency of water is a sensitive function of intermolecular interaction, it is evident that knowledge of the state of water in the membrane is vital for understanding proton conduction in proton exchange membranes. A full account of this work may be found in Z. Lu, G. Polizos, D. D. Macdonald, and E. Manias, "State of Water in Perfluorosulfonic Ionomer (Nafion 117) Proton Exchange Membranes", *J. Electrochem. Soc*, **155** (2), B163-B171 (2008).

Dielectric Relaxation Study of the Dimethyl Sulfoxide-Water System

Water is a highly self-associated liquid with an open, low coordination number structure; the coordination number is about 4.8 at 20 °C.[100] A number of models have been proposed to account for the physical properties of water.[101,102] Nevertheless, water remains an anomalous liquid, where no single model is able to explain all of its properties.[103] Ionic, polar, and hydrophobic solutes perturb the structure of water in different ways with profound consequences on their solubility, hydration thermodynamics, and their association with other solutes. Solute-induced perturbations in the water structure are, in turn, less understood than the structure of water itself, and has long been a subject of controversy in chemistry, biology, and physiology.[104]

In this section, we present and discuss results of a dielectric relaxation study of aqueous solutions of dimethyl sulfoxide (DMSO). The interest in DMSO is due, in part, to the wide use of DMSO-H_2O as solvents and reaction media. DMSO is a polyfunctional molecule with a highly polar S=O group and two hydrophobic CH_3 groups. The partial negative charge on the oxygen atom of DMSO molecule favors the formation of the hydrogen bonds with water molecules, while the non-polar CH_3 groups may give rise to hydrophobic hydration and hydrophobic association of DMSO molecules. Many observations[110,111] suggest that DMSO forms hydrogen bonds with water molecules throughout the whole composition range. Studies of the thermodynamic[108,109] and transport properties [11,12] of the DMSO/water system resulted in the generally accepted conclusion that, in the DMSO mole fraction range of 0.3-0.4, DMSO interactions with water, due to hydrogen bonding, are at a maximum.

The influence of DMSO on the molecular structure of liquid water has been studied by many authors, and a number of different and often mutually exclusive explanations exist in literature. The HH (water-H to water-H), MM (methyl-H to methyl-H) and the MH (methyl-H to water-H) pair correlation functions in DMSO/water mixtures have been measured by Luzar and coworkers[112-115] with neutron diffraction. The water structure is

found to be weakly affected by the presence of DMSO, but the percentage of water molecules that are hydrogen bonded to each other is substantially reduced compared to that in pure water. Furthermore, no evidence for hydrophobic association of DMSO molecules has been observed in DMSO/water mixtures, which is similar to the previous findings from IR spectroscopy of the OH and OD bands [116,117] and other experiments [118]. These results point to a "breaking" of water structure caused by the presence of DMSO molecules. Many other experiments, including temperature of maximum density measurements [119] and ionic conductance studies [120] also leads to the conclusion that small amounts of DMSO acts as a structure breaker in water. On the other hand, neutron inelastic scattering and X-ray diffraction studies [106] and NMR measurements[105.121] indicate that small amounts of DMSO increase the molecular order of water. Infrared spectroscopy [117] as well as density and partial molar volume measurements [122] show that small quantities of DMSO have little effect on the water hydrogen bonding. Computer simulations of the structure of DMSO/water mixtures have also been discussed on the basis of radial distribution functions.[114,123-131]. Typical molecular configurations, including DMSO.2H_2O clusters, have been revealed in the simulations. DMSO was found to "enhance" the structure of water in very dilute solutions, while a further increase in DMSO concentration in the solution led to a "breakdown" of the water structure. However, different explanations have been offered for the "enhancement" of water structure in the presence of very small amount of DMSO. Luzar et al.[113,114] attributed water structure enhancement to the association of water with the DMSO oxygen atom by strong hydrogen bonding, while Mancera et al.[126] claimed that it is due to the hydrophobic hydration of the methyl groups of DMSO.

So far, less attention has been given to highly concentrated DMSO solutions. Dimethyl sulfoxide is a self-associated liquid, reflected by its high mp (18.55 ^oC), bp (189.0 ^oC), and high molar entropy of vaporization (124 $J.K^{-1}.mol^{-1}$). Infrared and Raman studies[132-134] suggest the existence of dimers and higher polymers in liquid DMSO. A distinct anti-parallel ordering of the molecular dipoles has been observed by static permittivity measurements[135] and by molecular dynamics simulation.[123] In highly concentrated solutions, insufficient water molecules are available to completely hydrate the DMSO molecules. One would expect that it is solute-solute association that leads to the formation of microphases in these solutions. But, one can also imagine that molecular complexes are formed by hydrogen bonding between DMSO and water molecules. For example, a recent MD simulation [129,130] revealed the existence of 1H_2O-2DMSO cluster (an association of a pair of DMSO molecules through their oxygen atoms linked by one water molecule) in DMSO-rich mixtures.

Dielectric relaxation spectroscopy (DRS) probes the response of the total dipole moment of a system,, to a time-dependent external electrical field.[136] This inherent ability to monitor the cooperative motion of a molecular ensemble makes it a powerful tool for investigating liquids whose structure and dynamics are dominated by intermolecular hydrogen bonds. Dielectric relaxation measurements of DMSO/water mixtures have been the object of several investigations.[135,137,138] However, these data are still insufficient for a detailed analysis of the spectra with respect to the various questions raised. This mainly arises from the limited frequency and temperature ranges covered in these previous investigations.

In view of the inconclusive results of previous studies concerning the structure of dimethyl sulfoxide/water mixtures, it is appropriate to investigate the temperature dependence of the dielectric spectra of aqueous DMSO solutions over the whole composition range. Accordingly, in this study, we measured the dielectric relaxation spectra over a wide frequency range of 45 MHz - 26 GHz and at temperatures ranging from 25 to 45 ^{o}C. The aim of this work was to explore the relative contributions of the hydrophobic and hydrophilic groups of DMSO to modifying water structure, and to elucidate the structure of DMSO/water mixtures over the whole concentration range.

Dielectric spectra of dimethyl sulfoxide (DMSO)/water mixtures, over the entire concentration range, have been measured using the transmission line method at frequencies from 45 MHz to 26 GHz and at temperatures of 298–318 K. The relaxation times of the mixtures show a maximum at an intermediate molar fraction of DMSO. The specific structure of mixtures in different concentration regions was determined by the dielectric relaxation dynamics, obtained from the effect of temperature on the relaxation time. A water structure "breaking effect" is observed in dilute aqueous solutions. The average number of hydrogen bonds per water molecule in these mixtures is found to be reduced from that in pure water. The increase in the dielectric relaxation time in DMSO/water mixtures is attributed to the spatial (steric) constraints of DMSO molecules on the hydrogen-bond network, rather than being due to hydrophobic hydration of the methyl groups. The interaction between water and DMSO by hydrogen bonding reaches a maximum at DMSO molar fraction of 0.33, reflected by the maximum activation enthalpy for dielectric relaxation in this mixture, suggesting the formation of a stoichiometric compound, H_2O-DMSO-H_2O. In highly concentrated solutions, negative activation entropies are observed, indicating the presence of aggregates of DMSO molecules. A distinct anti-parallel arrangement of dipoles is obtained for neat DMSO in the liquid state according to the Kirkwood correlation factor (= 0.5), calculated from the static permittivity. The similarity of the dielectric behavior of pure DMSO and DMSO-rich mixtures suggests that dipole-dipole interactions contribute significantly to the rotational relaxation process in these solutions. A full account of this work may be found in Z. Lu, E. Manias, D.D. Macdonald, M. Lanagan, "Dielectric Relaxation in Dimethyl Sulfoxide/Water Mixtures Studied by Microwave Dielectric Relaxation Spectroscopy," *J. Phys. Chem*. A, **113**, 12207-12214 (2009).

3. Synthesis of new proton-conduction polymers and membranes derived from the polyphosphazene system. (H. R. Allcock with D. K. Lee: Chemistry Department, in collaboration with P. Hammond and coworkers, M.I.T. Chemical Engineering Department)

Rationale

The search for new proton conductive polymer membranes is driven by several realities. First, the polymer must bear acidic groups to promote proton transmission. Second, it must be stable to highly acidic media. Third, to conduct protons via the conventional mechanism, it should be a phase-separated material with both hydrophilic and hydrophobic domains. However, the last factor is one of the major reasons why existing commercial membranes cannot be used above 100^{o}C except under pressure. Proton conduction via the Grotthus mechanism requires the presence of free water in the

membrane, and volatilization of the water at temperatures above 100°C reduces the proton conduction significantly.

Thus, the design of membranes that function at elevated temperatures has to involve the search for new materials based on new chemistry that favor proton transmission at much lower water concentrations than are currently typical. This is the reason for the research described in the preceding two sections of this report. The study of a low level of proton conduction via **bound** water in an amphiphilic membrane, as discussed in the first section of this report, is of considerable significance, and this provides clues about possible lines of synthetic investigation for the future.

Design and Synthesis of Novel PEMs

Two alternative approaches to the development of new polymer electrolyte membranes are: (1) to assemble composite membranes from pre-existing polymers to combine the physical attributes of one polymer with the proton conduction of the other, or (2) to synthesize new polymers that bear both acidic functional groups and hydrophobic units and then convert the resultant polymers to membranes. The first approach has the advantage that pioneering polymer synthesis is not required. The second approach involves major challenges in synthesis chemistry, but offers the prospect of major breakthroughs. Both approaches have been explored and are described below.

(1) Composite membranes derived from layered films of two different macromolecules. The development of new membranes that conduct ions (including protons) at low water levels will require an approach that is drastically different from those that have been pursued in the past. One non-conventional approach is to produce multi-layer membranes in which the ions are transferred directly from site to site without the involvement of water.

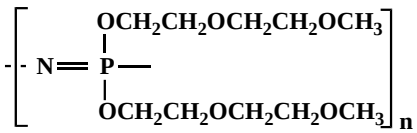

MEEP

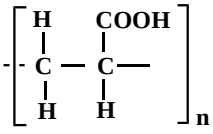

Poly(acrylic acid)

This approach was not part of our original proposal, but an investigation of it was considered to be sufficiently important to warrant our immediate attention. To explore this possibility we have collaborated with the group of Prof. Paula Hammond in the Chemical Engineering Department at M.I.T.[139] This group has in-depth experience with the fabrication of multi-layer membranes. The logic behind this project is to use a known anhydrous ion-conductive polyphosphazene, poly[bis(methoxyethoxyethoxy)-phosphazene (MEEP), in conjunction with poly(acrylic acid) to produce multi-layer assemblies and to monitor the cation transport of these membranes.

The oxygen atoms in the MEEP side chains have the ability to hydrogen bond to the carboxylic acid protons of poly(acrylic acid). This provides a mechanism for the transport of protons across a membrane without the participation of water.

Layer-by layer (LbL) assembly is a versatile thin-film fabrication method that consists of the repeated, sequential immersion of a substrate into aqueous solutions of complementary functionalized polymers. To the best of our knowledge, this is the first incorporation of a polyphosphazene into a multilayer structured thin film. Because the film deposition takes place from aqueous media, it is possible to monitor proton conductivity as the water content is progressively reduced and thus ascertain the possibility for water-free or low water proton conduction.

These films show controlled thickness growth, high ionic conductivity, and excellent hydrolytic stability. The ionic conductivity of these films was studied by changing the assembly pH of initial polymer solutions and thereby controlling the hydrogen bonding characteristics. Despite similar film composition, MEEP/PAA LbL films assembled at higher pH values have enhanced water uptake and transport properties, which play a key role in increasing ion transport within the films. At fully humidified conditions, the ionic conductivity of MEEP/PAA is 7×10^{-4} S cm^{-1}, over one order of magnitude higher than previously studied hydrogen bonded LbL systems. Finally, free standing films were isolated from low-energy surface substrates, which allows for bulk characterization of these thin films.

Experimental technique. Assembly of the LbL films was completed by using a programmable ZEISS DS50 slide stainer. To construct LbL films, substrates (glass, patterned ITO, polystyrene, or ZnSe) were first immersed in aqueous MEEP solution (10 mM calculated based on the repeat unit) for 20 minutes, followed by three two minute rinses in water, and then in PAA (10 mM) for 20 minutes followed by three two minute rinses in water. The pH of both polymer solutions and rinse baths were identical and adjusted prior to assembly by adding 1M HCl solution dropwise. The dipping process was repeated numerous times to produce a film of desired thickness. The free-standing films were peeled off from polystyrene substrates.

For in-plane conductivity measurements, LbL films deposited on microscope slides (VWR) were placed in a conductivity cell with platinum wires as the electrodes, and tested in a humidity and temperature controlled chamber (Electro-tech Systems, Inc.). Relative humidity was controlled down to 10% RH, and dry (0%RH) measurements were performed in a nitrogen-filled glove box with <1 ppm water content. Through-plane conductivity measurements were performed by depositing LbL films on patterned ITO substrates (Delta Technologies), and gold electrodes were thermally evaporated (~100nm) on the multilayers. The active area was 6 mm^2. Ionic conductivity values were determined by electrochemical impedance spectroscopy with a Solartron 1260 impedance analyzer by sweeping the frequency from 1 MHz down to 1 Hz.

Results. MEEP was synthesized by the reaction of poly(dichlorophosphazene) with the sodium salt of methoxyethoxyethanol, followed by purification by dialysis against water.

The ionization degree of PAA was controlled during thin-film assembly by systematically varying the assembly pH from 3.50 down to 2.00 for all polymer and rinse solutions. In all cases, the MEEP/PAA films grow linearly up to as many as 75 bilayers across the entire assembly pH range. Figure 7 shows the bilayer thickness of MEEP/PAA films as a function of assembly pH. The maximum bilayer thickness is greater than 200 nm/bilayer at the lowest assembly pH values, and is significantly reduced down to 50 nm/bilayer at the assembly pH =3.5. Large bilayer pair thicknesses are commonly observed in hydrogen bonded multilayer thin films due to looser network formed between weakly associative groups; furthermore, the potential for dimerization between PAA sidegroups increases the chance of greater amounts of film deposited with each cycle.

Because the MEEP/PAA system relies on hydrogen bonding to build the film, the degree of ionization in PAA greatly affects the bond attractions and like-charge repulsion between the polymer chains. At low pH, the ethyleneoxy side chains of MEEP paired with the carboxylic acid groups of PAA to create enough hydrogen bond crosslinks between layers to stabilize the resulting film. By changing the pH of the assembly baths, this cross-linking attraction can be varied, thus changing the stability of the film and allowing tuning of the final thickness. At higher pH values, the adsorbed PAA layer becomes increasingly thinner, as hydrogen bonding between PAA side chains (acid-acid dimerization) is decreased. The LbL film growth is suppressed at assembly pH values above pH=3.5 due to the more highly ionized PAA, which introduces large electrostatic repulsion, and limits the hydrogen bonding interaction between MEEP and PAA.

Figure 1 also shows the tunability of the ionic conductivity of MEEP/PAA films by varying the assembly pH. In-plane conductivity was measured at fully humidified conditions at 25 °C using platinum wires one centimeter apart on the surface of a 50 bilayer MEEP/PAA film. By increasing the assembly pH, the bulk proton conductivity increases from $1x10^{-4}$ S cm^{-1} at assembly pH =2.0 up to $7x10^{-4}$ S cm^{-1} at assembly pH = 3.5. This increase could be partially attributed to the higher ionization of PAA (more anionic sites for ion transport); however, the effect of ionization on proton conductivity is small as verified by the values obtained from pristine PAA films, and cannot account for the 7-fold increase observed for the LbL assembled films. Therefore, the observed enhancement of conductivity is due to the changes in the effective hydrogen bond network and/or composition in the films built at higher pH values, and resulting differences in ion and water transport. We hypothesize that the average number of transient hydrogen bonds per unit volume should undergo an overall decrease with these small increases in pH. The observed trend is consistent with the conductivity trend observed for the previously assembled LbL PEO/PAA systems, with MEEP/PAA values consistently being higher than the PEO/PAA values obtained at 100% RH.[16]

To determine the impact of ambient humidity on the ionic conductivity, 25 bilayers of MEEP/PAA films were assembled on patterned ITO/Glass substrates followed by thermal gold evaporation on top of the film to yield an 8-cell ITO | MEEP/PAA | Au configuration. Through-plane conductivity measurements were then carried out by connecting the ITO and gold ends to the impedance analyzer. Figure 2 shows the ionic conductivity values of MEEP/PAA multilayers assembled at pH = 2.5 (circles) and pH = 3.0 (triangles) as the

%RH is decreased from 60% down to 0%. In agreement with conductivity measurements taken at fully humidified conditions, LbL films assembled at high pH values yield higher values, presumably due to a more favorable, loose polymer network for ion and water transport, which would facilitate ion conduction via Grotthuss and carrier mechanisms. On the other hand, it is important to note that the difference in ionic conductivity between these two films becomes systematically less pronounced at drier conditions, namely at %RH values less than 20%, and that the ionic conductivities converge in the dry state to the value of 10^{-9} S cm^{-1}. We attribute this behavior to the crucial role of water in ion transport of hydrated ethyleneoxy based systems and the impact of its relative uptake in the films on the mobility of the ionic species. As the films approach the dry state, the differences in hydrogen bond network become irrelevant; the rate-determining factor for these systems in the dry state is the inherent mobility of the ethyleneoxy chain segments in the matrix.

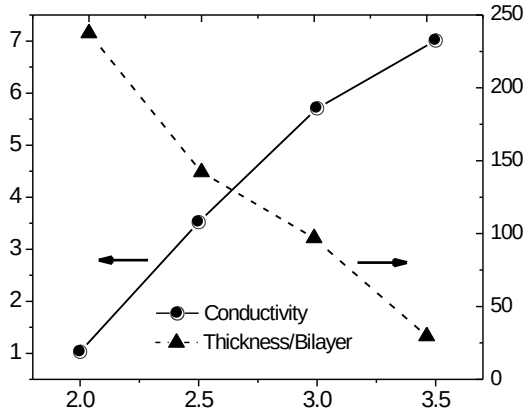

Figure 7. The assembly pH dependence of ionic conductivity at 100% RH (circles) and bilayer thickness (triangles).

Finally, to observe the effect of a small molecule plasticizer in a water-free environment, a drop of propylene carbonate was added onto a dry MEEP/PAA film (assembly pH =2.5) placed in a glovebox. The ionic conductivity rapidly increased by three orders of magnitude to reach 1.43 x 10^{-6} S cm^{-1} (Figure 8, empty circle) due to the more favorable liquid-like medium for ion transport. However, it is important to note that this value is still much lower than that of a film in fully humidified conditions indicating the crucial impact of water on proton transport through hydrated hydronium ions.

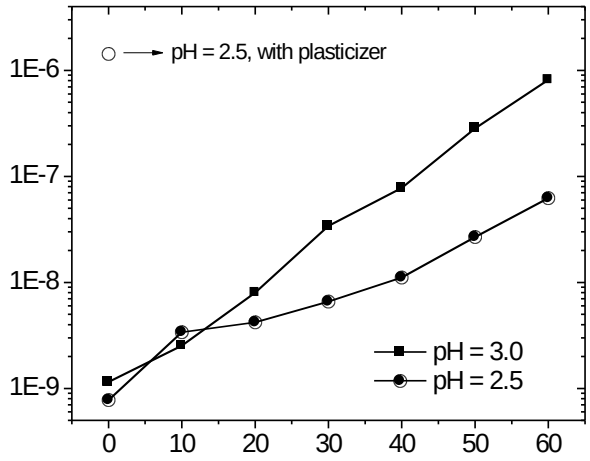

Figure 8. The relative humidity dependence of ionic conductivity of MEEP/PAA films assembled at pH = 2.5 and pH = 3.0. Also shown is the conductivity enhancement of a dry film upon addition of a small molecule plasticizer (propylene carbonate).

To analyze the thermal and mechanical characteristics, MEEP/PAA films were deposited on low surface energy polystyrene substrates and gently peeled off with tweezers. The resulting amber-colored and transparent films, indicated a homogenous laminate with minimal surface roughness. DSC thermograms for a peeled-off MEEP/PAA film assembled at pH = 2.5, were compared with spun-cast films of neat PAA and MEEP from water (Figure 9). The Tg values for pristine PAA and MEEP were found to be 76.0 °C and -80.5 °C, respectively. All MEEP/PAA LbL films exhibited a single T_g between that of neat MEEP and PAA, which is indicative of a truly homogeneous blended film. Interestingly, the observed T_g of MEEP/PAA LbL systems show little or no variation when the pH of the assembly solutions was varied over the range of 1.8 – 3.0. All MEEP/PAA samples assembled at pH values varying from 2.0 to 3.5 exhibited a T_g of -28.0 ± 2.0 °C. For this polymer pair, a Tg of -28.0 °C corresponds to a composition of 52 wt% MEEP or 21 mol% MEEP by use of the Fox equation. For the MEEP systems, the changes in intra- versus inter-molecular hydrogen bonding also seem to be responsible for changes in conductivity; however, the cause is not due to significant changes in relative MEEP content, which suggests that both the PAA and the MEEP adsorbed layers become thinner with higher pH. This difference between PEO and MEEP may be due in part to structural differences; the ethylene oxide groups attached as side chains to MEEP are very short, and would not undergo significant conformational changes to yield dense, loopy arrangements of PEO during the adsorption cycle, as anticipated with PEO when hydrogen bonding with PAA is optimized. In this case, less PAA adsorbed in the first adsorption cycle of the LbL assembly leads to lowered MEEP adsorption in the second. It is also noted that the relative increase in ionic conductivity with pH is also more moderate than observed with PEO/PAA, indicative of the smaller differences in the composition and structure of the films with pH. The primary reason for the observed increases in conductivity are therefore likely to be due to the higher number of charged sites available in the film and the decrease in the number of hydrogen bonds acting as effective physical crosslinks in the network, yielding a “looser” network and increased ion mobility.

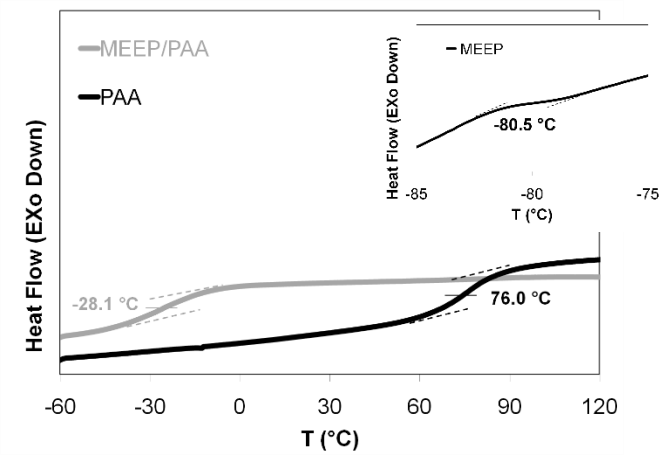

Figure 9. DSC thermogram for a free-standing MEEP/PAA film assembled at pH = 2.5, along with neat PAA and MEEP (inset). All MEEP/PAA LbL films displayed one T_g indicative of a homogenous blend. MEEP/PAA films assembled at different pH values showed little change in T_g.

A major concern for polymer electrolytes with low glass transition temperatures is their gum-like nature, which prohibits them from qualifying as *truly* solid-state electrolytes. To demonstrate the mechanical advantage of LbL assembled systems compared to pristine films of MEEP and PEO, we have tested the indentation response of MEEP/PAA films on glass as well as the pristine MEEP and PAA films for comparison. To minimize the substrate interference, we have assured that the thickness of the polymer film is at least ten times greater than that of the indentation distance. Preliminary results show that a typical MEEP/PAA film (~6 μm) yields an elastic modulus value of 690 ± 57 MPa at ambient conditions, over an order of magnitude higher than a pristine MEEP film (56 ± 5 MPa). We are currently investigating to verify these values by measuring the tensile strength of free-standing LbL films.

Water Transport. We utilized a recently developed approach to determine the water uptake and transport of MEEP/PAA LbL films with a quartz crystal microbalance (QCM).[22,23] This QCM method has been used to determine the permeability of various gases through polymer thin films, coatings and powders. QCMs measure the change in mass per unit area of a sample by measuring the variation in frequency of a quartz resonator due to absorption and diffusion of the permeating species, in this case water, in the films. Permeability is defined as:

$$P = \frac{J \cdot l}{\Delta p} = S \cdot D \qquad (1)$$

where J, l, and Δp are the flux, film thickness, and partial pressure difference across the film, respectively. Analyzing water permeation through a film involves both an equilibrium thermodynamic property, solubility (S), and a kinetic property, the diffusion coefficient (D). Both parameters, S and D, can be obtained from mass uptake experiments using the QCM. The ability to control the relative humidity of the QCM sample chamber allows the study of the relationship between water transport in MEEP/PAA films and the dependence of humidity on ionic conductivity.

To investigate the water uptake characteristics, MEEP/PAA films (5-10 bilayers, 0.5 – 2.1 μm) were assembled on quartz crystals and equilibrated at 30 °C under a dry nitrogen atmosphere until there is no longer a loss in moisture from the film, as determined by QCM. Then, the films were exposed to a step change to 100%RH while monitoring the changes in oscillation frequency. Figure 10a shows the water uptake of two MEEP/PAA films upon exposure to a fully humidified environment followed by a step change back to dry nitrogen and the corresponding water loss. Water uptake as a function of incremental step changes in humidity is shown in Figure 10b. The kinetic data from the single step experiment allows for the calculation of the diffusion coefficient through use of a simplified model of one-dimensional diffusion of water into a slab.

The linear sorption isotherm from the multi-step experiment yields the films' solubility. The permeability of the film is simply calculated from Equation 1 as the product of solubility and the diffusion coefficient. It is important to note that while deviations from the Sauerbrey Equation can exist for highly hydrated films, these deviations are minimal for thin films studied at the QCM's fundamental frequency (5 MHz).

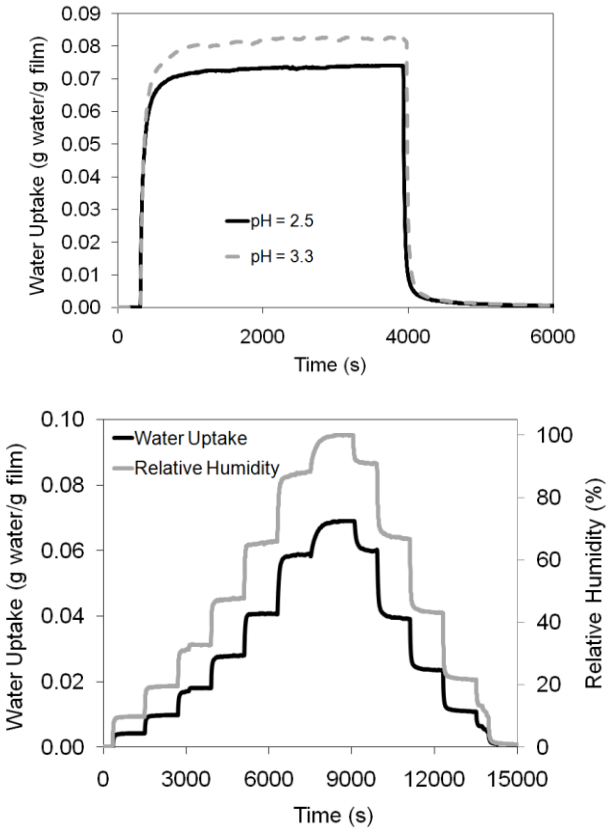

Figure 10. (a) Water vapor uptake and desorption as a function of time for MEEP/PAA LbL films assembled at pH=2.5 and pH=3.3 at 30°C. A step change in the sample chamber relative humidity from 0 to 100% occurs at t=300 s, while a step change from 100 to 0% occurs at t=3900 s. (b) Water vapor sorption isotherm at 30°C for a MEEP/PAA film assembled at pH=2.5.

The solubility values, diffusion coefficients, and permeability values of water in MEEP/PAA LbL films, along with neat, spun-cast MEEP and PAA films, are given in Table 1. PAA has a water uptake value of 0.111 g H_2O/g PAA, which corresponds to 0.32 water molecules per PAA repeat unit, while MEEP uptakes 0.027 g H_2O/g MEEP or 0.38 water molecules per MEEP repeat unit. The water transport properties of PAA are in agreement with literature;[23,26] however, the water uptake of MEEP is lower than previously reported values and may be attributed to differences in film processing. The water uptake of the MEEP/PAA LbL films is between that of MEEP and PAA, which is expected because the LbL films are homogenous blends of the two polymers. MEEP/PAA films assembled at pH 3.3 absorb 22.7% more water on a gravimetric basis than pH 2.5 films, most likely due the increased charge on the incorporated PAA at pH 3.3. Overall, in the case of MEEP/PAA LbL systems, films assembled at higher pH values have larger diffusion coefficients and solubilities. For example, MEEP/PAA films assembled at pH 3.3 have diffusion coefficients approximately 30 times larger and solubility values about 25% larger than films assembled at pH 2.5; thus, films assembled at pH 3.3 have water permeability values 35 times higher than films assembled at pH 2.5. The increase in water transport properties at higher pH values is consistent with the increase in ionic conductivity values of MEEP/PAA films at higher pH values, especially under humidified conditions. Regardless of the mechanism of ion transport through a polymer electrolyte, an increase in the water transport properties will result in higher ionic conductivities when the membrane is humidified. Thus, the increase in ionic conductivity values of MEEP/PAA films assembled at higher pH values is attributed to better water transport, which is improved by a looser hydrogen bond crosslinked network and the increased presence of some ionized PAA groups.

Table 1. Diffusion coefficients, solubilities, and permeabilites of water in MEEP/PAA films assembled at pH=2.5 and pH=3.3, along with neat MEEP, PAA and LbL assembled PEO/PAA films (T = 30°C).

Polymer	**H_2O Uptake** (g H_2O/g film)	**D** (cm^2/s)	**S** (cm^3 H_2O/cm^3 film cmHg)	**P** (Barrer)
MEEP	0.027	1.31E-13	17.5	10.0
PAA	0.111	3.72E-13	70.6	0.03
MEEP/PAA (pH = 2.5)	0.066	1.72E-11	41.7	7.17
MEEP/PAA (pH = 3.3)	0.081	4.84E-10	52.8	255
PEO/PAA (pH = 2.5)[23]	0.090*	1.3E-11	28.1	36

Barrer = 10^{-10} cm^3 (STP) cm cm^{-2} s^{-1} $cmHg^{-1}$ *70% RH

The water transport in MEEP/PAA LbL films and previously assembled PEO/PAA LbL films both assembled at pH 2.5 compares quite closely, [23] with MEEP/PAA having a slightly higher permeability value, indicating more favorable water transport characteristics. While the functional groups of MEEP and PEO are the same, the water transport properties might also be influenced by the nature of the hydrogen bonded network formed in each case by LbL assembly. MEEP, which presents ethylene oxide groups as side chains, may form a relatively stronger LbL hydrogen bonded network as compared to the ethylene oxide groups contained in the backbone of PEO.

Summary. The layer-by-layer assembly of MEEP/PAA thin films has been demonstrated by utilizing the hydrogen bonding between these two polymers. The ionic conductivity of these films is tuned by changing the assembly pH of initial polymer solutions and thereby controlling the hydrogen bonding characteristics. The growth rate of these films can be tuned over the range of < 50 nm/bilayer up to > 200 nm/bilayer, which is quite large for an LbL assembled system. At fully humidified conditions, the ionic conductivity of MEEP/PAA is over one order of magnitude higher than previously studied hydrogen bonded LbL systems (~7 x 10^{-4} S cm^{-1}). This improvement in conductivity is attributed to both MEEP's superior ion transport properties and the high water transport of these blends. Using the LbL technique to tune the properties of the film is promising to obtain stable and high performance solid state electrolytes for various electrochemical energy applications. At fully dry conditions, ionic conductivity values of these films show little variation with respect to assembly conditions due to the films' similar morphology and composition, as evidenced by bulk characterization of free-standing films. Free standing films are isolated from low-energy surface substrates, which allowed for bulk characterization of thin films with DSC. Indentation experiments show that the elastic modulus of MEEP/PAA is over an order of magnitude higher that neat MEEP, which is critical for the applications of solid polymer electrolyte systems. The kinetic and thermodynamic data obtained allows for a full characterization of water solubilities, diffusion coefficients, and permeability.

(2) Design and synthesis of alternative proton-conduction polymers. The rationale for this research is to use a synthetically highly versatile polymer system - the polyphosphazene platform - to explore new chemistry that could lead to the preparation of improved proton-conduction membranes.

Two of the advantages of the polyphosphazene system are the ease of modification of the polymers and their stability under aggressive conditions. Properties can be fine tuned to achieve desired characteristics by facile macromolecular substitution reactions carried out on the parent reactive intermediate, poly(dichlorophosphazene). This provides access to a large number of polymer architectures with different side groups. Furthermore, the polyphosphazene backbone is stable toward oxidation, which is a considerable advantage compared to the use of conventional organic polymers as fuel cell membranes. As a starting point, the synthesis of a polyphosphazene with a similar architecture to Nafion was attempted (Figure 11). We and others had shown in earlier work[140-146] that sulfonated, phosphonated, or sufinimidated aryloxyphosphazene polymers were a good starting point for alternative fuel cell membranes. These polymers are phosphazene equivalents of Radel

membranes in the sense that they are prepared by post-synthesis sulfonation or phosphonation of hydrophobic aryl-based polymers. In the work described here the objective was to investigate some variations on the polyphosphazene side group structure in an attempt to set the stage for the preparation of membranes that functioned with low water content.

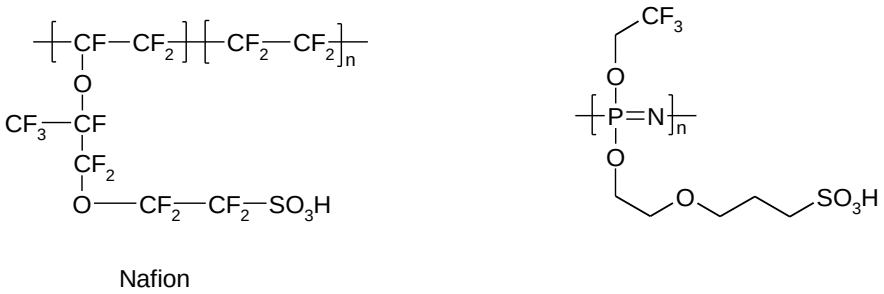

Figure 11: Structure of Nafion and one of the proposed polyphosphazenes.

Nafion consists of a hydrophobic poly(tetrafluoroethylene) backbone with fluorinated etheric side chains that are terminated by hydrophilic sulfonic acid groups. When swelled with water, the dual component Nafion forms nanometer-wide water channels, which are crucial for proton conduction. The proposed polyphosphazene analogues would also contain hydrophobic and hydrophilic components, which should form phase-separated domains when swelled by water. Possible hydrophobic side groups are trifluoroethoxy, higher fluoroalkoxy, phenoxy or phenylphenoxy units (Figure 12). The hydrophilic side groups consist of an etheric side chain terminated by a sulfonic acid group.

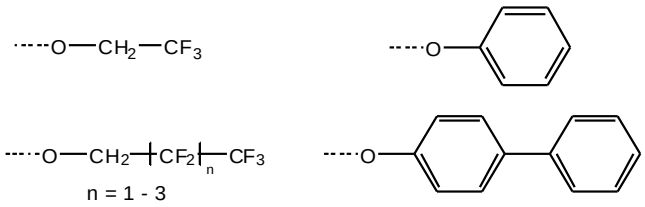

Figure 12: Hydrophobic side groups.

The main challenge in the synthesis of sulfonated polyphosphazenes lies in the incorporation of sulfonic acid groups into the side units. Traditional methods for introducing sulfonic acid functionality into the side group structure utilize aggressive sulfonating agents such as concentrated sulfuric acid[140] or sulfur trioxide. These sulfonating agents cause cleavage of the phosphazene backbone unless the backbone is protected by bulky hydrophobic side groups. Thus, initially we explored at a preliminary level several alternative synthetic techniques for the incorporation of sulfonic acid groups into the side chains of polyphosphazenes. These methods include (a) non-covalent protection of the sulfonic acid before the side unit is linked to the backbone, (b) radical sulfonation of vinyl groups in side groups already attached to the backbone, and (c) ring opening of a sultone. The first two methods were not successful, but the initial results for method (c) show promise. The details of each method are discussed below.

Initially, a 'noncovalent protection' method that had been reported in the literature was examined using dimethyldipalmitylammonium bromide to couple phenyl sulfonic acid groups to poly(dichlorophosphazene).[147] This method was used to protect an etheric side group with a sulfonic acid functionality (Reaction 1). However, numerous attempts to characterize the protected product by NMR techniques and by mass spectrometry left doubts about the utility of this method for the system studied. A possible explanation may lie in the stronger acidity of aryl sulfonic acid groups compared to alkyl sulfonic acid groups.

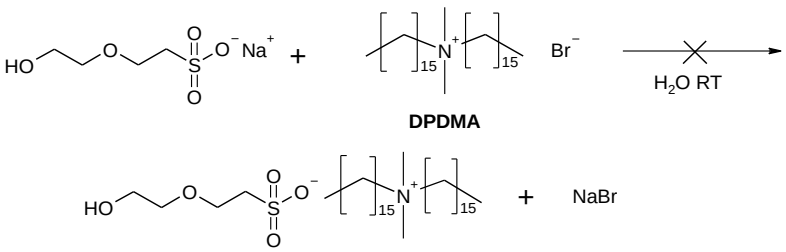

Reaction 1: Non-covalent protection method of sulfonic acid.

Alternative routes for introducing sulfonic acid groups to polyphosphazenes were then investigated. The first employed the radical addition of a sulfate group to a double bond. This procedure was adapted from a method reported by Weinreb who sulfonated vinyltrimethylsilane using sodium bisulfite and a radical initiator.[148] Usually, radical addition to double bonds occurs in an anti-Markovnikov fashion. However, radical sulfonation of ethylene glycol vinyl ether gave a Markovnikov product (Reaction 2), probably formed due to the stabilization of the radical intermediate by the etheric oxygen. By using 2-allyloxyethanol, in which the double bond is separated from the oxygen by a carbon spacer, an anti-Markovnikov product was obtained (Reaction 3). However, this sulfonation method was unsuccessful (Reaction 4) when the same side chain was connected to a small molecule model cyclic trimeric phosphazene or high polymeric phosphazenes.

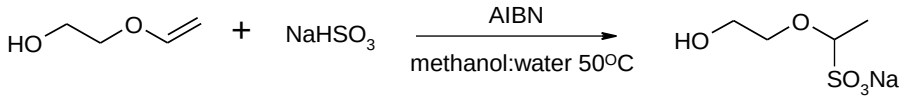

Reaction 2: Markovnikov product from ethylene glycol vinyl ether.

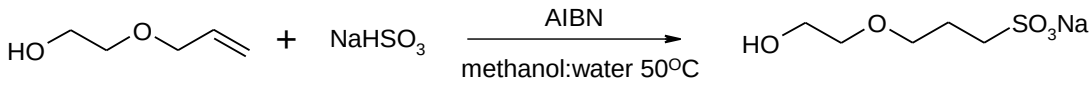

Reaction 3: Anti-Markovnokov product from 2-allyloxyethanol.

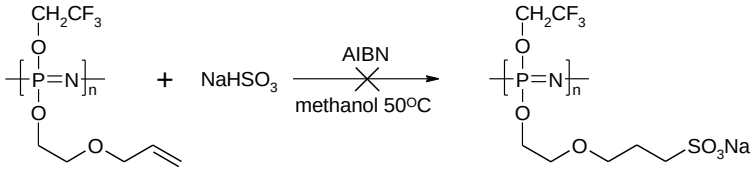

Reaction 4: Radical sulfonation of phosphazenes.

Possible reasons for this problem could be the presence of trace amounts of unreacted P-Cl bonds, or that the reactions with higher molecular weight substrates are unusually slow.

The most recently studied route employed to introduce sulfonic acid groups involves the ring opening of a sultone to yield a sulfonic acid group. This method has been used by us previously to introduce sulfonic acid groups into small molecule cyclic phosphazenes and to high molecular weight polyphosphazenes which contained terminal amino groups. However, the same method had not been attempted with phosphazenes that contain terminal hydroxyl groups. In test reactions, when sodium phenolate was allowed to react with 1,3-propane sultone, the sultone ring opened to form a sulfonic acid-terminated alkyl chain (Reaction 5). Similar reactions carried out on a model phosphazene cyclic trimer were also successful. (Reaction 6). Hexa(p-allyloxyphenoxy)cyclotriphosphazene was synthesized and the allyl group was subsequently cleaved with a palladium catalyst form the hydroxyl group. The hydroxyl group was allowed to react with 1,3-propane sultone yielded the sulfonated phosphazene. Similar reactions at the high polymeric phosphazene level provide an attractive option for future work.

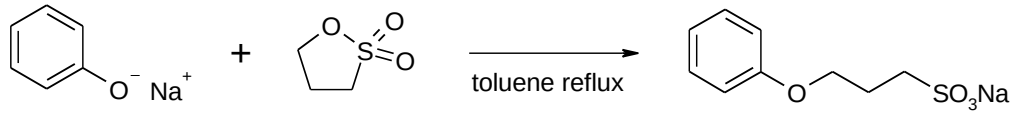

Reaction 5: Sultone ring opening reaction.

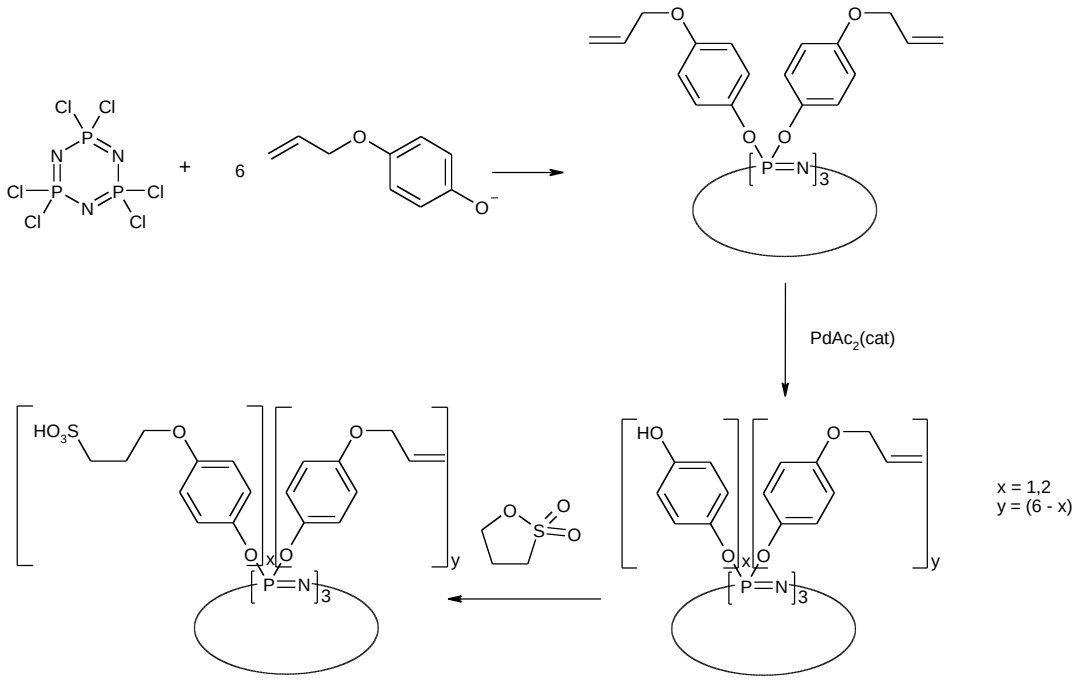

Reaction 6: Model sultone ring opening reaction on cyclic phosphazene trimer.

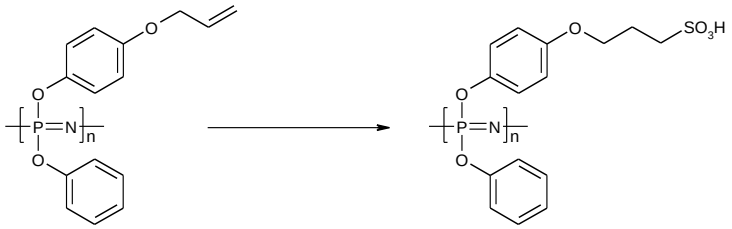

Reaction 7: Sultone ring opening reaction on polymer.

In spite of the possibility that this last method can be used to produce proton conduction membranes, we concluded from stability studies that the presence of a non-fluorinated alkyl side chain was detrimental to the long-term viability of a membrane. Consequently we believe that the most useful method for the functionalization of polyphosphazenes for fuel cell purposes is via the direct sulfonation of aryloxy-substituted polymers using methods that we and others pioneered earlier.[142-146] However, the chain cleavage known to occur during this process needs to be avoided by modifications to the sulfonation process. What should be done in future work is to combine the attributes of aryloxy groups as platforms for sulfonation with fluorinated side groups, which are among the most hydrophobic entities. Both side groups can be present on the same polymer chain either in blocks or as random co-substituted species, and preliminary experiments are underway to develop this approach. Moreover, we conclude that **surface** sulfonation reactions are more likely to produce strong membranes than the conventional solution processes. Suggestions for implementing this approach are given below.

Recommendations for Future Research

1. Characterization of the State of Water in Proton Conducting Membranes by NMR T_1 Relaxation

We have devoted considerable effort to define more precisely the T_1 value of solid-like water in Nafion in order to calculate accurately the distribution of solid and liquid water. A T_1 value of around 26 ms at room temperature is obtained consistently regardless of the drying methods, such as dry freezing or vacuum drying over P_2O_5. The value of 26 ms is a high T_1 value compared to typical T_1 values of solid water as found in kanemite, Zeolite A, and other polymers such as starch, cellulose and in sulfonimido polyphosphazenes. The room temperature T_1 relaxation times for solid water in these systems are typically around 4-8 ms at depending on the magnetic field. Kohlrausch-stretched exponential plots of the T_1 inversion recovery curves indicate that the T_1 value consists of a single component. There are two possible explanations for the different T_1 relaxation values of dried Nafion. One is that even at the low water content obtained over P_2O_5, there may still be some liquid water present in Nafion, trapped between the polymer chains. Although the Kohlrausch plots indicate a single component, fast exchange between bound water and trapped water would give the same result. Moreover, water contained in "Teflon-like" hydrophobic channels may be even more mobile than "normal" liquid water since there are fewer hydrogen bonds restricting the water movement in the hydrophobic environment. Studies of water molecules trapped in hydrophobic environments such as carbon nanotubes show that water molecules adopt a gas like behavior due to lack of hydrogen bonding. [18] This would lead to a longer T_1 value for the water in a hydrophobic environment compared to normal liquid water, which in fast exchange with the "bound" water would increase the T_1. A second possibility is that the bound water in the vicinity of the sulfonic acid groups experiences a very different type of motion than has been observed previously.

Several experiments have been planned to study the long T_1 relaxation of bound water in Nafion. First, we plan to attempt to incorporate D_2O into poly(tetrafluoroethylene) (PTFE) to study the interaction of water with the hydrophobic chains. This will be challenging because no ionic interactions will be present to stabilize water molecules within the hydrophobic environment. Furthermore, unlike Nafion, PTFE is highly crystalline and penetration of water between the polymer chains will be difficult. We will attempt to incorporate water within the polymer by melting PTFE powder and D_2O in a sealed chamber. Alternatively, D_2O hydrated salts or zeolites can be embedded in PTFE. The studying T_1 NMR relaxation times of D_2O incorporated in the hydrophobic environment of PTFE might elucidate the results that we have obtained.

Characterization of the state of water should also be extended to other fuel cell membranes. The fuel cell membranes that are under consideration are sulfonated poly(arylene ether sulfone) (BPSH), sulfonated pole(arylene thioether sulfone) (PATS) and sulfonated polyimide sPI copolymers. (Figure 9) These polymers have a different morphology compared to Nafion and provide a good comparison for the study of the state of water in fuel cell membranes.

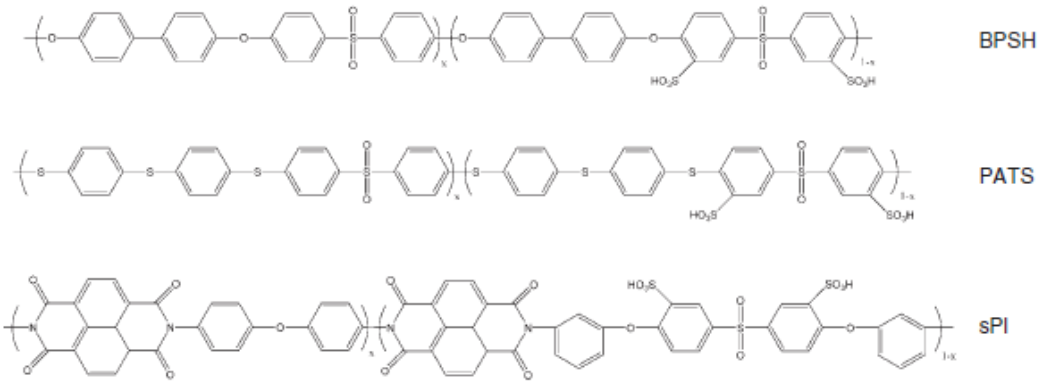

Figure 7: Chemical structures of commonly studied organic proton conducting membranes.

2. Dielectric Relaxation Studies

In the future, the mechanism of proton conduction and the state of water in PEMs should be explored by measuring the activation parameters for the conduction process and by measuring dielectric relaxation spectra to ascertain rotational relaxational frequencies. This can be done by measuring the conductivities of PEMs as a function of temperature, pressure, and water content and by determining the transference number, also as a function of water content, temperature, and pressure. The volume of activation can be extracted from the differential of ln(σ) with respect to pressure.

$$\left(\frac{\partial \ln(\sigma)}{\partial P}\right)_T = -\frac{\Delta V^{o,\#}}{RT}$$

The measurements can be made using standard conductivity cells contained within a pressure vessel capable of holding pressures up to 1,000 bar (≈ 15,000 psi). The same apparatus provides a means to determine the pressure-dependence of the rotational relaxation time of water. The conductivity cells will be calibrated using KCl solutions and data in the literature.

The transport properties of the membranes used in this work can be explored in an autoclave capable of withstanding temperatures and pressures to 200 ºC and 1000 bar, respectively. The autoclave should be pressurized using an ENERPAC hand pump, with a silicone oil being the pressurizing fluid. The impedance of the membrane can be measured via a four point contact method using a Solartron Model 1255 Frequency Response Analyzer (FRA) coupled to a Solartron Electrochemical Interface (EI). The impedance will be measured over the frequency range of 100 KHz to 0.001 Hz using a small excitation voltage (20 mV, peak-to-peak). The transference numbers are accessible using Wagner's method by analyzing the transient in current produced in response to a step in the voltage imposed across the membrane. Stainless steel can be used as the blocking electrodes. The experimental set-up is shown schematically in Figure 14. The transmission line contains the sample under investigation, and the impedance of the transmission line is measured

over a wide frequency range of 100 MHz to more than 100 GHz. The measured impedance data are then processed to yield the dielectric constant and the dielectric loss. Details of this calculation can be found in the paper by Lu, et.al., and will not be repeated here. It is sufficient to note that the method has been thoroughly tested and found to be accurate. As with the electrochemical studies referred to above, the test cell (transmission line in the case of the dielectric studies) can be contained within a pressure vessel that is capable of being pressurized to 1000 bar at temperatures up to 200 ^{o}C. The transmission line itself will be contained within a polyethylene bag so as to separate the cell from the pressurizing fluid. The activity of water can be controlled using hydroscopic salts or pure water, as desired.

3. Design and Synthesis of Novel PEMs

Imidazole and triazole containing polyphosphazenes. Future work should investigate the synthesis of anhydrous proton conducting phosphazene membranes. Polymers currently used in anhydrous proton conduction membranes often contain imidazole or triazole groups. The presence of these side groups allows protons to conduct in a Grotthus chain mechanism without the presence of water molecules. Therefore, these membranes can operate at temperatures that are above the boiling point of water. Possible synthetic routes are discussed below.

There are two factors to consider when linking an imidazole group to polyphosphazenes. First, the nitrogen at the 1 position of the imidazole ring must be protected to prevent direct attachment of the imidazole ring to the phosphazene backbone. Second, a proton at the 2 position of the imidazole ring is fairly acidic and must be blocked to prevent side reactions. Therefore, the side group shown is an appropriate unit for reaction with poly(dichlorophosphazene).

Triazole-containing polyphosphazenes are also attractive materials as anhydrous proton conducting membranes. Triazoles, like imidazoles, are also able to conduct protons by the Grotthuss mechanism. A possible synthetic approach involves attachment to the phosphazene backbone of an alkyne group which is then converted to a triazole group through click chemistry. Preliminary reactions to synthesize imidazole- and triazole-containing side groups have confirmed the feasibility of this strategy.

Surface-type reactions to produce acid-functionalized polymers. An entirely different strategy for the preparation of sulfonated fluorocarbon-phosphazene proton conduction membranes is worth exploring. This would involve **surface** sulfonation rather than molecular-level sulfonation. By this means, it is possible to restrict the sulfonation processes to the interfacial region of a polymer thereby preserving the chain lengths and strength of the internal regions.

Specifically, an approach is to fabricate fluoroalkoxy and fluoroaryloxy phosphazene polymers in the form of thin films that contain a second phase. The second phase would be micro- or nanoscale fibers of a material that can be dissolved or etched away by sulfuric acid. Typical second phase fiber materials are poly(vinyl alcohol), poly(ethylene oxide), cellulose, nylon, and so on. Nanofibers can be produced by

electrostatic spinning. The composite of the polyphosphazene and fibers could then be solution-cast as films or melt fabricated. Treatment with fuming or concentrated sulfuric acid should sulfonate both the surface and the walls of the tunnels left after erosion of the fibers. The resultant material would consist of a hydrophobic matrix penetrated by hydrophilic, sulfonated channels. The membranes can then be evaluated as produced or can be heat annealed to allow reorganization of both hydrophilic and hydrophobic regions. An alternative is to synthesize amphiphilic phosphazene block copolymers, allow these to undergo phase separation, and then permit sulfonation to occur via the hydrophilic regions.

Acknowledgements

We thank Professor Qiming Zhang from the Department of Electrical Engineering at Penn State for providing samples of Aquivion, and Dr Wenbin Luo for her help with NMR experiments. We are also indebted to Professor Paula Hammond, Dr. Avni A. Argun, Nathan Ashcraft, and Marie Herring for their work with the LbL membranes. Collaborations with Drs. Zijie Lu, Evangelos Manias, Michael Lanagan, and George Pozlios are also acknowledged.

References in the Text

Part 1

1. Mauritz, K. A.; Moore, R. B. *Chem. Rev.*, **2004**, *104*, 4535-4585

2. Kreuer, K. D. *Chem*. *Mater*.**1996**, *8*, 610-6413.

3. Lakshmanan, B.; Huang, W.; Olmeijer, D.; Weidner, J. W. *Electrochem. Solid-State Lett*. **2003**, *6*, A282– A285

4. Rozière, J.; Jones, D. J. *Annu. Rev. Mater. Res*. **2003**, *33*, 503– 555

5. Mathias, M. F.; Makharia, R.; Gasteiger, H. A.; Conley, J. J.; Fuller, T. J.; Gittleman, C. J.; Kocha, S. S.; Miller, D. P.; Mittelsteadt, C. K.; Xie, T.; Yan, S. G.; Yu, P. T. *Interface* **2005**, *14*, 24

6. Gasteiger, H. A.; Kocha, S. S.; Sompalli, B.; Wagner, F. T. *Applied Catalysis B: Environmental*, **2005**, *56*, 9-35

7. Wang, B *Journal of Power Sources* **2005**, *152*, 1-15

8. G. Scharfenberger, W. H. Meyer, G. Wegner, M. Schuster, K.-D. Kreuer, J. Maier *Fuel Cells*, **2006**, *6*, 237-250

9. Subbaraman, E.; Ghassemi, A.; Zawodzinski, T. A. *J. Am. Chem. Soc*., **2007**, *129*, 2238-2239

10. Celik, S. U.; Aslan, A.; Bozkurt, A. *Solid State Ionics*, **2008**, *179*, 683-688

11. Park, M. J.; Downing, K. H.; Jackson, A.; Gomez, E. D.; Minor, A. M.; Cookson, D.; Weber, A. Z.; Balsara, N. P. *Nano Lett.* **2007**, *7*, 3547-3552

12. Matsumura, S.; Hlil, A. R.; Lepiller, C.; Gaudet, J.; Guay, D.; Shi, Z.; Holdcroft, S.; Hay, A. S. *Macromolecules* **2008**, *41*, 281– 284

13. Roy, A.; Yu, X.; Dunn, S.; McGrath, J. E. *J. Membr. Sci*. **2009**, *327*, 118– 124

14. Saito, T.; Moore, H. D.; Hickner, M. A. *Macromolecules* **2010**, 43, 599-601.

15. Bae, B.; Miyatake, K.; Watanabe, M *Macromolecules*, **2010**, *43*, 2684–2691

16. Kreuer, K. D. *J. Membr. Sci*. **2001**, *185*, 29-39

17. Ioselevich, A. S.; Kornyshev, A. A.; Steinke, J. H. G. *J. Phys. Chem. B*, **2004**, *108*, 11953–11963

18. Yang, Y. S.; Siu, A.; Peckham, T. J.; Holdcroft, S. In *Polymers for Fuel Cells 1*; Scherer, G. G. Ed; *Advances in Polymer Science vol. 215*; Springer: Berlin, **2008**, 55-126

19. Lu, Z.; Polizos, G.; Macdonald, D. D.; Manias, E. *Journal of The Electrochemical Society*, **2008**, *155*, B163-B171

20. Paddison, S.J.; Reagor, D.W.; Zawodzinski, T.A. *J. Electroanal. Chem.*, **1998**, *459*, 91–97

21. Kim, Y. S.; Dong, L.; Hickner, M. A.; Glass, T. E.; Webb, V.; McGrath, J. E. *Macromolecules*, **2003**, *36*, 6281–6285

22. Elomaa, M.; Hietala, S.; Paronen, M.; Walsby, N.; Jokela, K.; Serimaa, R.; Torkkeli, M.; Lehtinen, T.; Sundholmc, G.; Sundholm, F. *J. Mater. Chem.*, **2000**, *10*, 2678-2684

23. Laporta, M.; Pegoraro, M.; Zanderighi L. *Phys. Chem. Chem. Phys.*, **1999**, *1*, 4619-4628

24. Ye, G.; Jansen, N.; Goward, G. R. *Macromolecules* **2006**, *39*, 3283-3290

25. MacMillan, B.; Sharp, A. R.; Armstrong, R. L. *Polymer*, **1999**, *40*, 2471–2480

26. Kreuer, K. D.; Paddison, S. J.; Spohr, E.; Schuster, M. *Chem. Rev.*, **2004**, *104*, 4637-4678

27. Paddison, S. J. *Annu. Rev. Mater. Res.*, **2003**, *33*, 289-319

28. Benesi, A. J.; Grutzeck, M. W.; O'Hare, B. V.; Phair, J. W. *Langmuir*, **2005**, *21*, 527-529

29. O'Hare, B; Grutzeck, M. W.; Kim, S. H.; Asay, D. B.; Benesi, A. J. *J. Magnetic Resonance*, **2008**, *195*, 85-102,

30. Benesi, A. J.;O'Hare, B.; Grutzeck, M. W.; Phair, J. W. *Journal of Physical Chemistry B*, **2004**, *108*, 17783-17790

31. Park, S.; Venditti, R. A.; Abrecht, D. G.; Jameel, H.; Pawlak, J. J.;Lee, J. M. *Journal of Applied Polymer Science*, **2006**, *103*, 3833-3839

32. D. Radloff, C. Boeffel, W. H. Spiess *Macromolecules* **1996**, *29*, 1528-1534

33. Bunce, N. J.; Sondheimer, S . J.; Fyfe, C. A. *Macromolecules*, **1986**, *19*, 333–339

34. Geil, B.; Kirschgen, T. M.; Fujara, F. Physical Review B, 2005, 72, 014304-1−014304-10

35. Schmidt-Rohr, K.; Spiess, H. W. *Multidimensional Solid-State NMR and Polymers*; Academic Press: San Diego, CA, 1994.

36. Hoatson, G. L.; Vold, R. L. In *Encyclopedia of Nuclear Magnetic Resonance*; Grant, D. M., Harris, R. K., Eds.; Wiley & Sons Scientific: New York, 1996; p 1582

37. Dyck, A.; Fritsch, D.; Nunes, S. P.; *Journal of Applied Polymer Science*, **2002**, 86, 2820-2827

38. Perrin, J. C.; Lyonnard, S.; Guillermo, A.; Levitz, P *J. Phys. Chem. B*, **2006**, *110*, 5439–5444

39. ASTM Standard E104-02 "Standard Practice for Maintaining Constant Relative Humidity by Means of Aqueous Solutions," **2007**, ASTM International, West Conshohocken PA

40. Majsztrik, P. W.; Satterfield, M. B.; Bocarsly, A. B.; Benziger, J. B. *Journal of Membrane Science*, **2007**, *301*, 93-106

41. Kreuer, K. D.; Schuster, M.; Obliers, B.; Diat, O.; Traud, U.; Fuchs, A.; Klock, U.; Paddison, S. J.; Maier, J *Journal of Power Souces*, **2008**, *178*, 499-509

42. Pushpa, K. K.; Nandan, D.; Iyer, R. M. *J. Chem. Soc., Faraday Trans. 1*, **1988**, *84*, 2047-2056

43. Lindsey, C. P.; Patterson, G. D. *J. Chem. Phys.* **1980**, *73*, 3348-3357

44. Eikerling, M.;Kornyshev, A. A.;Kuznetsov, A. M.;Ulstrup, J.;Walbran, S. *J Phys Chem B* **2001**, *105*, 3646-3662

45. (a) Pokras, S. M. Investigation of the State of Water Adjacent to Solid Surfaces using Deuterium NMR. Honors Thesis [Online], The Pennsylvania State University, University Park, PA, April 2010 http://honors.libraries.psu.edu/theses/approved/WorldWideIndex/EHT-427/index.html (accessed July 2010)
(b) Slipak, S. H. Investigation of the State of Water Adjacent to Solid Surfaces using Deuterium NMR Spectroscopy. Honors Thesis [Online], The Pennsylvania State University, University Park, PA, April 2010 http://honor .libraries.psu.edu/theses/approved/WorldWideIndex/EHT-170/index.html (accessed July 2010)

46. Chen, R. S.; Jayakody, J. P.; Greenbaum, S. G.; Pak, Y. S.; Xu, G.; McLin, M. G.; Fontanella, J. J. *J. Electrochem. Soc.*, **1993**, *140*, 889-895

47. Zawodzinski, T. A.; Derouin, C.; Radzinski, S.; Sherman, R. J.; Smith, V. T.; Springer, T. E.; Shimshon, G. *J. Electrochem. Soc.*, **1993**, *140*, 1041-1047

48. Paddison, S. J. *J. New Mater. Electrochem. Systems*, **2001**, *4*, 197-207

49. Hickner, M. A.; Fujimoto, C. H.; Cornelius, C. J. *Polymer* **2006**, 47, 4238-4244.

50. Takimoto, N.; Wu, L.; Ohira, A.; Takeoka, Y.; Rikukawa, M. *Polymer*, **2009**, *50*, 534-540

Part 2

51. K. D. Kreuer, in *Handbook of Fuel Cells Fundamentals, Technology and Applications*, Vielstich, W.; Lamm, A.; Gasteiger, H. A., Eds., John Wiley & Sons: Chichester, U.K., 2003, vol. 3. Chapter 3

52. R. J. Mortimer and A. Beech, *Electrochim. Acta.*, **47**, 3383 (2002).

53. H. Michishita, H. Matsumoto, and T. Ishihara, *Electrochem.*, **76**, 288 (2008).

54. W. Y. Hsu, and T. D. Gierke, *J. Membr. Sci.*, **13**, 307 (1983).

55. K. D. Kreuer, *J. Membr. Sci.*, **185**, 29 (2001).

56. K. A. Mauritz and R. B. Moore, *Chem. Rev.*, **104**, 4535 (2004).

57. M. Doyle and G. Rajendran, in *Handbook of Fuel Cells Fundamentals,Technology and Applications*, Vielstich, W.; Lamm, A.; Gasteiger, H. A. Eds., John Wiley & Sons: Chichester, U.K., 2003, vol. 3, Chapter 30.

58. R. Paul and S. J. Paddison, *J. Phys. Chem. B*, **108**, 13231 (2004).

59. R. Paul and S. J. Paddison, *J. Chem. Phys.*, **123**, 224704 (2005).

60. S. J. Paddison, R. Paul, and T. A. Zawodzinski, Jr, *J. Electrochem. Soc.*, **147**, 617 (2000).

61. Z. Lu, G. Polizos, D. D. Macdonald, E. Manias, *J. Electrochem. Soc.*, **155**, B163 (2008).

62. M. Eikerling, A. A. Kornyshev, A. M. Kuznetsov, J. Ulstrup, and S. J. Walbran, *J. Phys. Chem. B*, **105**, 3646 (2001).

63. M. Eikerling and A. A. Kornyshev *J. Electroanal. Chem.*, **502**, 1 (2001).

64. M. Saito, N. Arimura, K. Hayamizu, and T. Okada *J. Phys. Chem. B*, **108**, 16064 (2004).

65. S. J. Paddison and R. Paul, *Phys. Chem. Chem. Phys.*, **4**, 1158 (2002).

66. K. D. Kreuer, S. J. Paddison, E. Spohr, and M. Schuster, *Chem. Rev.*, **104**, 4637 (2004).

67. A. A. Kornyshev, A. M. Kuznetsov, E. Spohr, and J. Ulstrup, *J. Phys. Chem. B*, **107**, 3351 (2003).

68. K. A. Mauritz, *Macromolecules*, **22**, 4483 (1989).

69. Z. D. Deng and K. A. Mauritz, *Macromolecules*, 25, 2739 (1992).

70. C. Tsonos, L. Apekis, and P. Pissis, *J. Mater. Sci.*, **35**, 5957 (2000).

71. C. Tsonos, L. Apekis, and P. Pissis, *J. Mater. Sci.*, **33**, 2221 (1998).

72. J. Baker–Jarvis, M. D. Janezic, and R. G. Geyer, *IEEE Trans. Instrum. Meas.*, **43**, 711 (1994).

73. Y. Wei and S. Sridhar, *IEEE Tran. Microwave Theory Tech.*, **39**, 526 (1991).

74. Y. Wei and S. Sridhar, *J. Chem. Phys.*, **92**, 923 (1990).

75. D. K. Misra, *Microw. Opt. Technol. Lett.*, **11**, 183 (1996).

76. S. J. Paddison, D. W. Reagor, and T. A. Zawodzinski, Jr., *J. Electroanal. Chem.*, **459**, 91 (1998).

77. S. J. Paddison, G. Bender, K. D. Kreuer, N. Nicoloso, and T. A. Zawodzinski, Jr., *J. New Mater. Electrochem. Syst.*, **3**, 291 (2000).

78. S. Jenkins, T. E. Hodgetts, R. N. Clarke, and A. W. Preece, *Meas. Sci. Technol.*, **1**, 691 (1990).

79. J. Baker-Jarvis, E.J. Vanzura, and W. A. Kissick, *IEEE Trans. Microwave Theory Techn.*, **38**, 1096 (1990).

80. L. Carrette, K.A. Friedrich, U. Stimming, *Fuel Cells*, **1**, 1 (2001)

81. R.W. Kopitzke, C.A. Linkous, H.R. Anderson, G.L. Nelson, *J. Elecctrochem. Soc.*, **147**, 1677 (2000)

82. P.D. Beattie, F.P. Orfino, V.I. Basura, K. Zychowska, J.F. Ding, C. Chuy, J. Schmeisser, S. Holdcroft, *J. Electroanal. Chem.*, **503**, 45 (2001)

83. B. Pivovar, Y. Wang, E.L. Cussler, *J. Membr. Sci.*, **154**, 155 (1999)

84. D. Rivin, C.E. Kendrick, P.W. Gibson, N.S. Schneider, *Polymer*, **42**, 623 (2001)

85. J. Kim, B, Kim, B. Jung, *J. Membr. Sci.*, **207**, 129 (2002)

86. T.A. Zawodzinski, T.E. Springer, J. Davey, R. Jestel, C. Lopez, J. Valerio, S. Gottesfeld, *J. Electrochem. Soc.*, **140**, 1981 (1993)

87. X. Ren, S. Gottesfeld, *J. Electrochem. Soc.*, **148**, A87 (2001)

88. T.D. Gierke, G.E. Munn, F.C.J. Wilson, *J. Poly. Sci., Polym. Phys.*, **19**, 1687 (1981)

89. W.Y. Hsu and T.D. Gierke, *J. Membr. Sci.*, **13**, 307 (1983)

90. M. Falk, *Can. J. Chem.*, **58**, 1495 (1980)

91. E.E. Boakye and H.L. Yeager, *J. Membrane Sci.*, **69**, 155 (1992)

92. Yu.S. Kim, L. Dong, M.A. Hickner, T.E. Glass, V. Webb, J.E. McGrath, *Macromolecules*, **36**, 6281 (2003)

93. F.X. Quinn, E. Kampff, G. Symth, V.J. McBrierty, *Macromolecules*, **21** 3192 (1988)

94. G. Symth, F.X. Quinn, V.J. McBrierty, Macromolecules, **21**, 3198 (1988)

95. R.M. Hodge, T.J. Bastow, G.H. Edward, G.P. Simon, A.J. Hill, *Macromolecules*, **29**, 8137 (1996)

96. H. Yoshida, Y. Miura, **J. Membr. Sci.**, **68**, 1 (1992)

97. K.A. Mauritz, Macromolecules 22 4483 (1989); Z.D. Deng, K.A. Mauritz, *Macromolecules*, **25**, 2739 (1992)

98. C. Tsonos, L. Apekis, P. Pissis, *J. Mater. Sci.*, **35**, 5957 (2000); *J. Mater. Sci.*, **33**, 2221 (1998)

99. S.J. Paddison, D.W. Reagor, T.A. Zawodzinski Jr., *J. Electroanal. Chem.*, **459**, 91 (1998)

100. D. Eisenberg, W. Kauzmann, *The Structure and Properties of Water*, Oxford University Press, Oxford, 1969.

101. G. W. Robinson, C. H. Cho, and J. Urquidi, *J. Chem. Phys.*, **111**, 698 (1999).

102. M. F. Chaplin, *Biophys. Chem.*, **83**, 211 (1999).

103. C. H. Cho, S. Singh, and G. W. Robinson, *Faraday Discuss*, **103**, 19 (1996).

104. G. W. Robsinson, S. B. Zhu, S. Singh, and M. W. Evans, *Water in Biology, Chemistry and Physics*, World Scientific Publishing Co. Ltd, Singapore, 1996

105. E. S. Baker and J. Jones, *J. Phys. Chem.*, **98**, 1730 (1985).

106. G. J. Stafford, P. C. Schaffer, P. S. Leung, G. F. Doebbler, G. W. Brady, and E. F. X. Lyden, *J. Chem. Phys.*, 50, 2140 (1969).

107. H. H.Szmant, in *Biological Actions of Dimethyl sulfoxide*, S.W. Jacob (Ed.), Ann. NY Acad. Sci., Vol. 243 Academic Press, New York, 1975.

108. J. M. G. Cowie and P. M. Toporowski, *Can. J. Chem.*, **39**, 2240 (1964).

109. M. F. Fox and K. P. Whittingham, *J. Chem. Soc., Faraday Trans.*, **75**, 1407 (1974).

110. J. Mazurkiewicz and P. Tomasik,. *J. Phys. Org. Chem.*, **3**, 493 (1990).

111. U. Kaatze, M. Brai, F. D. Sholle, and R. J. Pottel, *J. Mol. Liquid*, **44**, 197 (1990).

112. A. K. Soper and A. Luzar, *J. Chem. Phys.*, **97**, 1320 (1992).

113. A. K. Soper and A. Luzar. *J. Phys. Chem.*, **100**, 1357 (1996).

114. A. Luzar, A. K. Soper, and D. Chandler, *J. Chem. Phys.*, **99**, 6836 (1993).

115. J. T. Cabral, A. Luzar, J. Teixeira, and M. C. Bellissent-Funel, *J.Chem. Phys.*, **113**, 8736 (2000).

116. M. F.Fox and K. P. Whittingham, *J. Chem. Soc., Faraday Trans.*, **71**, 1407 (1975).

117. G. Brink and M. Falk, *J. Mol. Struct.*, **5**, 27 (1970).

118. J. T. W. Lai, F. W. Lau, D. Robb, P. Westh, G. Nielsen, C. Trandum, A. Hvidt and Y. Koga, *J. Solution Chem.*, **24**, 89 (1995).

119. D. D. Macdonald, M. D. Smith, and J. B. Hyne, *Can. J. Chem.*, **49**, 2817 (1971).

120. G. Petrella, M. Petrella, M. Castagnolo, A. Dell'Atti, and A. DeGiglio, *J. Solution Chem.*, **10**, 129 (1981).

121. K.Mizuno, S. Imafuji, T. Ochi, T. Ohta, and S. Maeda, *J. Phys. Chem. B*, **104**, 11001 (2000).

122. C. de Visser, W. J. M. Henvelsland, L. A. Dunn, and G. Somsen, *J. Chem. Soc., Faraday Trans.*, **74**, 1159 (1978).

123. I. I. Vaisman and M. L. Berkowitz, *J. Am. Chem. Soc.*, **114**, 7889 (1992).

124. A. Luzar and D. Chandler, *J. Chem. Phys.*, **98**, 8160 (1993).

125. A. Vishnyakov, A. P. Lyubartsev, and A. Laaksonen, *J. Phys. Chem. A*, **105**, 1702 (2001).

126, R. L. Mancera, M. Chalaris, and J. Samios, *J. Mol. Liquids*, **110**, 147 (2004).

127. M. Chalaris and J. Samios, *J. Mol. Liquids*, **98-99**, 399 (2002).

128. R. L. Mancera, M. Chalaris, K. Refson, and J. Samios, *J. Phys. Chem. Chem. Phys.*, **6**, 94 (2004).

129. I. A. Borin and M. S. Skaf, *J. Chem. Phys.*, **110**, 6412 (1999).

130. M. S. Skaf, *J. Chem. Phys.*, **107**, 7996 (1997).

131. Q. Zhang, X. Zhang, and D. X. Zhao, *J. Mol. Liquids*, **145**, 58; **145**, 67 (2009).

132. G. Fini and P. Mirone, *Spectrochim. Acta*, **32A**, 625 (1976).

133. M. I. S. Mastry and S. Singh, *J. Raman Spectrosc.*, **15**, 80 (1984).

134. C. Czeslik and J. Jonas, *J. Phys. Chem. A*, **103**, 3222 (1999).

135. U. Kaatze, R. Pottel, and M. Schafer, *J. Phys. Chem.*, **1989**, 93, 5623 (1989).

136. B. K. P. Scaife, *Principles of Dielectrics*, Clarendon Press, Oxford, 1998

137. A. K. Lyashchenko, A. S. Lileev, T. A. Novskova, and V. S. Kharkin, *J. Mol. Liquids*, **93**, 29 (2001).

138. J. J. Achadov, *Dielectric Properties of Binary Solutions*, Pergamon: Oxford, 1981

Part 3

139. A. A. Argun; J. N. Ashcraft; M. K. Herring; D. K. Y. Lee; H. R. Allcock; P. T. Hammond, Chem. Materials, 2010, 22, 226-232.

140. Allcock, H. R.; Fitzpatrick, R. J. *Chem. Materials* **1991**, 3. 1120-1132.

141. Allcock, H. R.; Hofmann, M. A.; Wood, R. M., Macromolecules **2001**, 34, 6915-6921.

142. Allcock, H. R.; Hofmann, M. A.; Ambler, C. M.; Lvov, S. N.; Zhou, X. Y.; Chalkova, E.; Weston, J. *J. Membrane Sci*. **2002**, 202, 47-54.

143. Allcock, H. R.; Hofmann, M. A.; Ambler, C. M.; Maher, A. E.; Wood, R. M.; Lvov, S.; Zhou, X. Y.; Chalkova, E.; Fedkin, M. W.; Weston, J. A. Chapter in special volume of *Polymers for Advanced Technology*, **2006**.

144. Hofmann, M. A.; Ambler, C. M.; Maher, A. E.; Chalkova, E.; Zhou, X. Y.; Lvov, S. N.; Allcock, H. R. *Macromolecules*, **2002**, 35, 6490-6493.

145. Allcock, H. R.; Wood, R. M., *J. Polymer Sci Part B, Polymer Physics*, **2006**, 44, 2358-2368.

146. Wycisk, R.; Pintauro, P. N.; Wang,W.; O'Connor, S. *J. Applied Polymer Sci*., **1996**, 1607–1617.
147. Weinreb, S. M.; Chase, C. E.; Wipf, R.; Venkatraman, *Organic Syntheses*, **2004**, 10, 707.